Quantum Mechanical Investigations on the Formation of Complex Organic Molecules on Interstellar Ice Mantles. Review and Perspectives

Quantum Mechanical Investigations on the Formation of Complex Organic Molecules on Interstellar Ice Mantles. Review and Perspectives

Journal:	*ACS Earth and Space Chemistry*
Manuscript ID	sp-2019-000827
Manuscript Type:	Review
Date Submitted by the Author:	01-Apr-2019
Complete List of Authors:	Rimola, Albert; Universitat Autonoma de Barcelona, Química Zamirri, Lorenzo; Universita degli Studi di Torino Dipartimento di Chimica, Chemistry Ugliengo, Piero; Universita degli Studi di Torino, Dipartimento di Chimica Ceccarelli, Cecilia; Univ. Grenoble Alpes, CNRS, Institut de Planétologie et d'Astrophysique de Grenoble (IPAG)

Quantum Mechanical Investigations on the Formation of Complex Organic Molecules on Interstellar Ice Mantles. Review and Perspectives

Lorenzo Zamirri,[1,2] Piero Ugliengo,[1,2] Cecilia Ceccarelli,[3] and Albert Rimola.[4*]

[1]*Dipartimento di Chimica, Università degli Studi di Torino, via P. Giuria 7, 10125, Torino, Italy*

[2]*Nanostructured Interfaces and Surfaces (NIS) Centre, Università degli Studi di Torino, via P. Giuria 7, 10125, Torino, Italy*

[3]*Univiversité Grenoble Alpes, CNRS, Institut de Planétologie et d'Astrophysique de Grenoble (IPAG), rue de la Piscine 414, 38000, Grenoble, France*

[4]*Departament de Química, Universitat Autònoma de Barcelona, 08193, Bellaterra, Catalonia, Spain*

*Corresponding author: albert.rimola@uab.cat

Abstract

The interstellar medium (ISM) is rich in molecules, from simple diatomic to complex organic ones, some of which have a biotic potential. A notable example, in this respect, is represented by the so-called interstellar complex organic molecules (iCOMs). Interestingly, the various phases involved in the formation of Solar-type planetary systems lead to an increasing chemical complexity, in which, at each step, more complex molecules form. In dark molecular clouds, dust grains are covered by ice mantles, mainly made up of H_2O but also of other volatiles species such as CO, NH_3, CO_2, CH_4 and CH_3OH. Although their mass is one hundred times lower than the gas-phase matter, these ice-covered grains play a fundamental role in the interstellar chemical complexity as some important reactions are exclusively catalyzed by their surfaces. For example, one of the current paradigms on the iCOMs formation assumes that iCOMs are synthesized on the ice mantle surfaces, in which reactants accrete and diffuse to finally react. As the usual approaches employed in astrochemistry (*i.e.*, spectroscopic astronomical observations, astrochemical modelling and laboratory experiments) cannot easily provide details on the iCOMs formation processes occurring on ice mantles at the atomic level, computational chemistry has recently become a complementary tool to fill in this gap. Indeed, it can provide an accurate description (*i.e.*, structures and reactive

energy profiles) of these processes. Accordingly, several recent studies simulating the formation of iCOMs on icy surfaces by means of quantum mechanical methods have appeared in the literature. This article aims to comprehensively review most of these works, focusing not only on standard iCOMs but also on simpler organic compounds as well as biomolecules. Perspectives on possible future directions of research using computational chemistry are also proposed.

1 Introduction

Despite the harsh conditions of the interstellar medium (ISM), more than 200 interstellar molecules have been discovered so far, with this number steadily increasing with time.[1] Among them, the class of C-bearing molecules with at least 6 atoms are defined as interstellar complex organic molecules (iCOMs).[2,3] Such a definition allows us to exclude simple molecules that are sure not *organic*, like H_2O, NH_3 or CO, but excludes some relevant ones like formaldehyde (H_2CO) and methanimine (CH_2=NH). Moreover, other species, although not being categorized as iCOMs, can play a crucial role in the organic, and eventually pre-biotic, chemistry occurring in the ISM, such as the case of formic acid (HCOOH), hydrogen cyanide/isocyanide (HCN/HNC) or the isocyanic acid (HCNO), just to mention a few.

Nonetheless, iCOMs have lately received a lot of attention for their potential contribution to the emergence of life and because iCOMs in solar-type hot corinos provide a direct link between interstellar chemistry and the small bodies of the Solar System, *i.e.* comets and asteroids.[4–6]

Although the presence of iCOMs has been known for decades,[7] the chemical routes that lead to their formation is still matter of intense debate. Two alternative paradigms are invoked in the literature: either iCOMs form in the gas-phase,[8–10] or on the interstellar grain surfaces.[8,11–13] Here, we will focus on the latter paradigm. Briefly, it postulates that iCOMs are synthesized on the grain surfaces following a three-step process: *i*) hydrogenation of frozen atoms and molecules to form saturated species (*e.g.*, CH_3OH from CO[14,15]) during the cold prestellar phase; *ii*) formation of radicals (*e.g.*, $CH_3O\cdot$, HCO·, $NH_2\cdot$) derived from the frozen hydrogenated species due to incidence of UV radiation and cosmic rays on the ice mantles, and *iii*) coupling of radicals to form iCOMs, in

which radicals are assumed to diffuse on the ice mantles due to temperature increase (≈30 K) during the protostellar phase.[11–13]

In this paradigm, therefore, interstellar grains play a major role, so we briefly describe their characteristics, in the context of this review. They are silicate and carbonaceous sub-micron size particles that permeate most of the Galaxy ISM.[16–18] In cold molecular clouds, grains are enveloped by iced mantles constituted mostly of water with smaller quantities of carbon monoxide and dioxide (CO, CO_2), ammonia (NH_3) and methanol (CH_3OH).[19,20] Therefore, when referring to grain surface reactions, what one really means is reactions occurring on surfaces of water ice.

Little is known about the structure of these iced mantles. Experiments evidenced similarities between the IR features of interstellar ices and those of amorphous solid water (ASW),[21] and accordingly they are usually referred to be amorphous and partly porous.[22] However, IR spectroscopy is not a definitive technique to derive conclusive structural features of these ices, as outlined in a recent work on the solid CO/H_2O interface.[23] From IR observations, it seems that ices present two different solid phases: *i*) a water-rich polar phase, most containing of iced H_2O, CO_2, NH_3 in direct contact with the silicate/carbonaceous core, and *ii*) an apolar phase, comprising most of the iced CO, the remaining CO_2 and probably most of the iced CH_3OH.

Investigating iCOMs has been carried out by means of the usual multidisciplinary approach applied in astrochemistry: astronomical spectroscopic observations, astrochemical models, and laboratory experiments. Spectroscopic observations can detect iCOMs in different astronomical sources and provide abundances in the different environments. However, they are not capable to give direct information on how iCOMs are formed, either on the grain-surfaces or in gas-phase. Astrochemical models are useful in rationalizing iCOMs observations. In these models, however, the energetic parameters introduced as input data are associated with some large and critical uncertainties (*i.e.*, in some cases they are derived from gas phase or empirical estimates) and, accordingly, predictions are uncertain too. As a matter of fact, current "grain-surface-formation" models are not capable to

reproduce the recent observations for methanimine and of methoxymethanol (CH_3OCH_2OH), where discrepancies of several orders of magnitude were reported.[6,24] Laboratory experiments are very useful in telling us the nature of the products formed but they are not able to reproduce realistically the physical conditions of the ISM (*e.g.*, the very low temperature and gas densities or the relatively high UV photon or H-atoms fluxes), as well as the chemical features of the ice grains such as the exact chemical composition.[25]

Within this context, computational chemistry is a complementary tool to the other approaches as it can alleviate part of the abovementioned problems. Computational simulations can furnish the atomistic and electronic structures of the systems under investigation, providing unique information such as structural, energetic and spectroscopic features of the ice mantles. They can also provide a molecular description of the elementary steps involved in a grain surfaces reaction (*i.e.*, adsorption/accretion, diffusion, chemical reactions and desorption) in which a full characterization of the energy profiles can be simulated. Interestingly, with these profiles, relevant energetic information of the grain surface process (*e.g.*, energy barriers, reaction rates, binding/desertion energies) can be obtained, which in turn can be used as accurate input data in the astrochemical models. However, this approach also holds some disadvantages: the main one is that results depend on both the method chosen to solve the equations describing the systems and the atomistic model adopted to represent the grain surface structure. In gas phase calculations this latter disadvantage is avoided, and hence different works dealing with the formation of iCOMs through gas phase processes are available in the literature, reporting accurate energy profiles and reaction rate coefficients.[26–33]

The very first computational chemistry works dealing with astrochemical reactions on ice surfaces date from the beginning of this century. However, the structural ice models were based on the presence of a limited number of H_2O molecules or implicit solvation models. It was not since the beginning of this decade that ice models started to be structurally more realistic, as periodic slab

models, amorphous systems, *etc*. Several works have covered the formation of interstellar molecules on grain surfaces. Some of them addressed the formation of simple compounds on dust grains, (*e.g*., H_2 and H_2O formation on silicates[34–37]), but most of them are related to the formation of iCOMs on ice mantles. The aim of the present work is to review all these later studies present in the literature, which to the best of our knowledge is hitherto fully missing. We only focus on computational works based on quantum (QM) or classical (MM) mechanics simulations, as these techniques are the most reliable ones to tackle iCOMs formation.

The review is organized as follows. Section 2 provides a description of the computational framework, focusing briefly on the quantum chemical methods and techniques, ways to calculate rate constants (including tunneling effects) and ice surface modelling strategies. Section 3 is the core of the review, in which the most relevant computational works dedicated to the "on-surface" iCOM formation are briefly exposed. Here, we are not limited to iCOMs according to the definition given above, but to also other related species, such as H_2CO, CH_3OH, and amino acids and nucleobases. Finally, Section 4 provides the conclusions including some future perspectives in the simulation of iCOMs formation on ice mantles by means of computational chemistry tools.

2 Computational Framework

2.1 Quantum mechanical methods

The chemical processes reviewed here concern a wide variety of reaction-types and mechanisms (proton/electron transfers, nucleophilic/electrophilic attacks, *etc*.) occurring at structural models mimicking the surfaces of interstellar ice mantles. Accordingly, accuracy of the results partly relies on the QM methodologies describing the chemical reactions.

When high accuracy is needed, approaches based on the improvement of the wavefunction such as the Møller-Plesset 2nd order perturbation theory and coupled cluster single, double and perturbative-triple electronic extrications method (namely, MP2 and CCSD(T), respectively) are adopted.[38,39]

However, these methods are extremely expensive for large systems and accordingly unpractical hitherto when modeling on-surface reactions. Alternatively, since the late 1990s, approaches based on the electron density, the so-called density functional theory (DFT) methods, have become computationally cheaper alternatives to the wavefunction-based ones, in which well-designed DFT methods provide acceptable accuracy.[40–44] Among them, the B3LYP, PBE and BHLYP functionals are three the of the most adopted DFT methods in QM calculations.

2.2 Potential Energy Surfaces

Potential energy surfaces (PESs) describe the energy of a system (collection of atoms) as a function of its geometry (the position of the atoms). Complete PESs are characterized by calculating the energy of the system as a function of the internal coordinates (bonds, angles and dihedrals). Stationary points (points with a zero gradient in the PES) have physical meaning (Figure 1A): minima correspond to physically stable chemical species (reactants, products and intermediates), while 1st order saddle points correspond to transition states (TSs), the highest energy points on the reaction coordinates (the lowest energy paths connecting reactants with products). All other stationary points (*i.e.*, higher order saddle points and maxima) are physically unsounded. When the PESs are described as a function of the reaction coordinate (the coordinate governing the reaction), the surface is called energy profile (see Figure 1B).

The nature of the stationary points can be known by diagonalizing the Hessian matrix of second derivatives of the potential energy with respect to the atomic positions. Hessian eigenvalues are related to the frequency vibrational modes of the system: for minima structures, all frequencies are real, while saddle points have one imaginary frequency.

Since QM calculations account for the electronic structure of the systems, exploration of PESs for reactions (in which chemical bonds break and form) has to be done within this framework (at variance with classical mechanics, which do not account for electrons).[45–47]

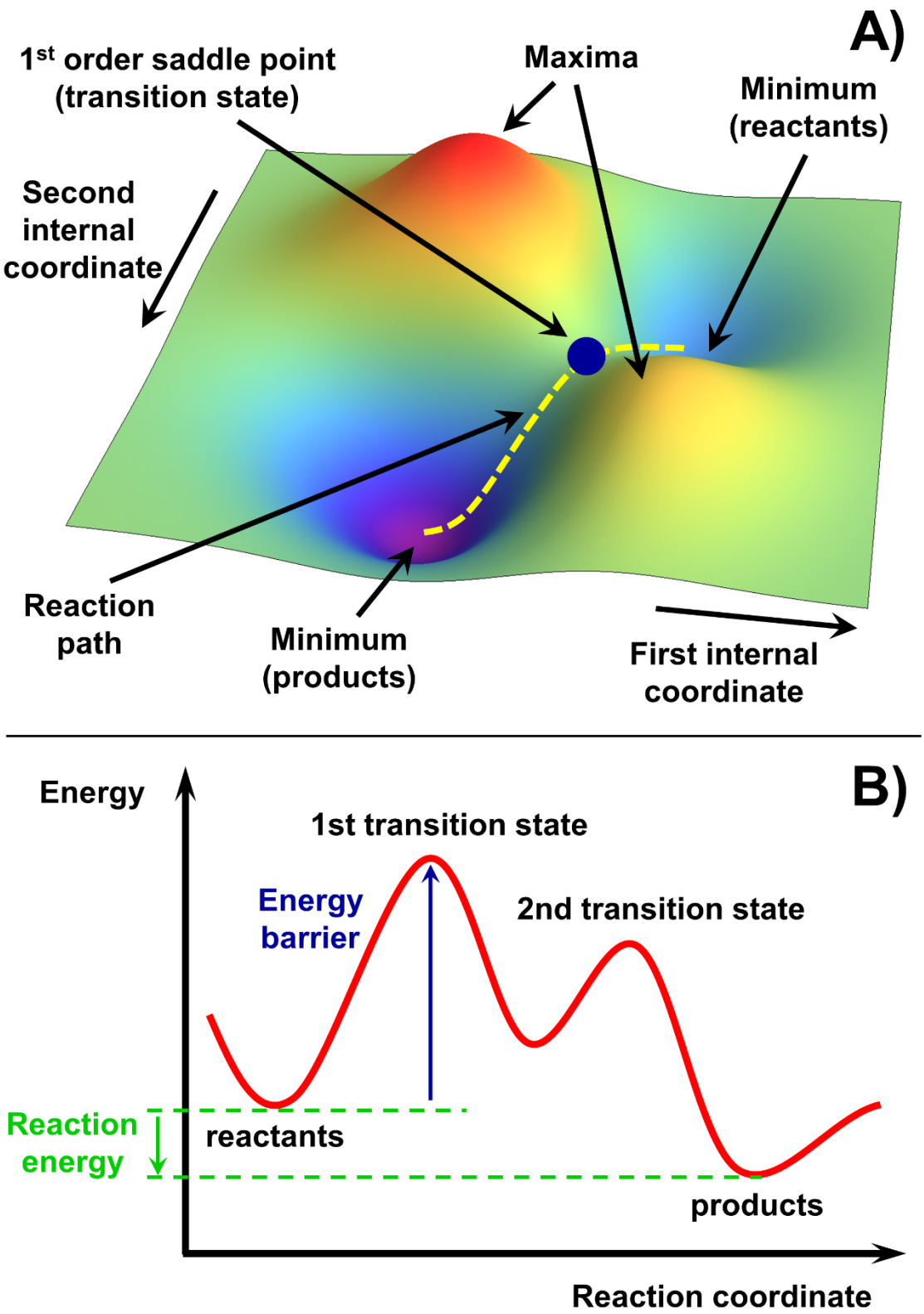

Figure 1. A) Example of a potential energy surface (PES) described as a function of two internal coordinates. The different stationary points are also shown: minima (reactants and products), 1st order saddle point (connecting the minima with the reaction path) and maxima (with no physical meaning). B) Example of an energy profile, in which the PES is described as a function of the reaction coordinate, with the different stationary points. The intrinsic energy barrier (in blue) and the reaction energy (in green) are also shown.

2.3 Static calculations versus dynamic simulations

Exploration of PESs is done systematically by solving the electronic Schrödinger equation for the different stationary points. These are called static calculations because dynamic effects inferred by temperature are not accounted for, *i.e.*, calculations are performed considering 0 K.

Dynamic simulations (also known as molecular dynamics simulations, MDs) allow studying of the evolution in time-space phase of the atomic positions subject to the internal forces of chemical nature and to the kinetic energy due to the temperature of the system. MDs simulations combining electronic structure theory (for electron description) with classical molecular mechanics (for the nuclei motion) are usually referred as *ab initio* molecular dynamics simulations (AIMDs). MDs are adaptable to very different situations: indeed, they can be used to transform a crystalline system into an amorphous one,[23,48] to sample the adsorbate/surface PES,[49] to study the diffusion properties of the adsorbates,[50] or to explore the role of temperature and pressure in surface phenomena.[51,52]

2.4 Kinetics

Reaction kinetics refers to the velocity of chemical reactions, which are quantified by the rate constant. Quantitatively, reaction rates can be derived from the classical "transition state theory" originally developed by Henry Eyring, Meredith G. Evans and Michael Polanyi in 1935.[53] Starting from the assumption of the existence of a "*quasi*-equilibrium" between reactants and TSs, the kinetic rate constant k of a given reaction can be derived as:[54,55]

$$k = \kappa \frac{k_B T}{h} e^{-\frac{\Delta G^{\neq}}{RT}} (c^0)^{1-m} \qquad \text{Eq. 1}$$

where κ is the transmission coefficient (for reactions without tunneling assumed to be 1), T the absolute temperature, k_B the Boltzmann constant, h the Planck constant, R the ideal gas constant, c^0 the standard concentration, m the molecularity ($m = 1$ or 2 for uni or bimolecular reactions) and $\Delta G^{\neq}$ the Gibbs free energy barrier, *i.e.* the free energy difference between the TS and the reactants.

For a unimolecular reaction ($m = 1$), k can be easily related to the half-life time $t_{1/2}$;[47] *i.e.*, the time needed to consume the half of the initial amount of reactants:

$$t_{1/2} = \frac{\ln 2}{k} = \frac{h}{\kappa k_B T} e^{\frac{\Delta G^{\neq}}{RT}} \ln 2 \qquad \text{Eq. 2}$$

At the very low temperatures of the ISM long half-life times are derived, even for very low energy barriers. The dependence of $\log(t_{1/2}/1\ \text{Myr})$ on $\Delta G^{\neq}$ for different typical temperatures of ISM is reported in Figure 2. Data shown in the inset clearly indicate that, in the 10-25 K temperature range of MCs,[56] only reactions with very low kinetic barriers can occur.

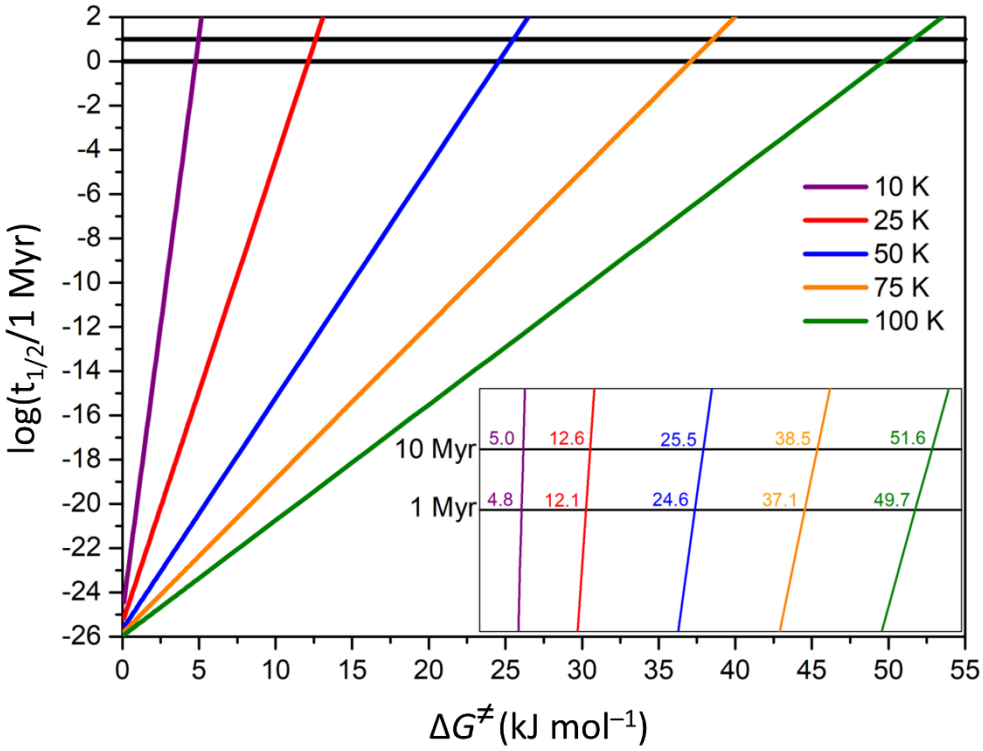

Figure 2. Dependence of the half-life time ($t_{1/2}$) with the free energy barrier ($\Delta G^{\neq}$) for a unimolecular reaction at different temperatures (in K). $t_{1/2}$ are normalized to 1 Myr. The two straight horizontal lines represent 1 and 10 Myr, respectively, taken as reference lifetimes of a typical molecular cloud.[57] Inset: zoomed view in the $-2 \leq \log(t_{1/2}/1\ \text{Myr}) \leq 2$ range. Numbers at the crossing points are the $\Delta G^{\neq}$ values at which $t_{1/2}$ equals 1 and 10 Myr, respectively.

It is worth mentioning that at the particularly low interstellar temperatures, and for not too high and wide barriers, quantum tunneling may play a prominent role favoring reaction rates. There are several ways to account for such tunneling effects,[58] such as the semi-classical approaches, in which

the the transmission coefficient κ is calculated through specific formulae (*e.g.*, the Eckart formula,[59] usually used in astrochemical modeling). More evolved is the instanton theory,[60,61] which is a derivation of the harmonic quantum transition state theory,[62] where the tunneling path is fully optimized in the Feynman-path-based instanton theory.[63] Few examples on the use of the instanton theory in astrochemical reactions can be found elsewhere.[64,65]

The free energy of a given species can be easily obtained once computed the partition functions (translation, rotational, electronic and vibrational) and applying statistical thermodynamics relations.[66] The free energy of a species at temperature T is given by:

$$G(T) = E + \zeta + \epsilon(T) + PV(T) - TS(T) \qquad \text{Eq. 3}$$

where E is the potential energy (electronic plus nuclear) of the species from the electronic structure calculation, ζ is the zero-point energy (ZPE), $\epsilon(T)$ is the thermal contribution to the internal energy (both terms obtained with frequency calculations), and P, V and S represent the volume, pressure and entropy, respectively. At the low temperatures of the ISM, the last three terms of Eq. 3 are small and usually neglected. Thus, energy profiles are usually presented in terms of E or $E + \zeta$, with the latter being referred to as "internal energy at 0 K" or, equivalently, "enthalpy at 0 K".

2.5 Surface Modeling

Accuracy of the theoretical results, in addition to the QM methods (see above), also relies on the specific models adopted to simulate the ice surfaces. Two strategies can be adopted to model the external surfaces of icy grains: the periodic approach and the cluster approach. The periodic approach consists of applying the periodic boundary conditions (PBC) into a unit cell containing the surface adsorptive/catalytic sites, resulting in an infinite 2D slab model, *i.e.*, periodicity is only applied in the two directions defining the unit cell (Figure 3A).[23,67–77] In contrast, the cluster approach consists of cutting out from the periodic model a finite set of atoms containing the surface sites, so that the surface is essentially modelled by a molecular system (Figure 3B).

Powerful computer codes have been developed over the years to solve the PBC problem for infinite systems. However, due to their infinite nature, application of highly accurate wave function-based methods is overwhelming (although recent developments indicate applicability for MP2[78]) and they can in practice only be studied using DFT methods. Moreover, localization of transition state structures is less developed compared to molecular codes, thus PES characterization being limited to "simple" reactions. On the contrary, a large variety of quantum molecular programs can properly handle cluster models, characterizing PESs of complex chemical reactions, using even CCSD(T), depending on the cluster size.

The cluster approach can be limited by: *i*) the need to ''heal'' dangling bonds resulting from cutting covalent/ionic bonds from the extended system, and *ii*) the size of the cluster, which should be large enough to include the catalytic sites. For this latter, cluster sizes can prohibitively be large, reducing the abovementioned advantages when adopting molecular computer codes. A possible solution is to use embedding techniques like the ONIOM method,[79–81] in which the region of interest (*e.g.*, the region close to the catalytic sites) is treated at high level of theory (MP2, CCSD(T)), whereas the surrounding region is treated at a lower level (DFT, semi-empirical or even molecular mechanics, Figure 3C).

Interstellar ices are usually reported to be highly amorphous and, partly, porous,[20,82–84] although the degree of porosity has recently been questioned.[22] Amorphous surfaces (Figure 3D) can be generated by amorphizing (*e.g.*, running MDs at high temperature) the slab model, or by cutting out a previously amorphized bulk system. The presence of pores can influence the reactivity on interstellar ices since: *i*) adsorbates can be entrapped and retained inside the pore (hence favoring reaction with other entrapped species), and *ii*) water molecules may exert a "solvent-like" effect, thus stabilizing intermediates or transition states. A consistent way to simulate pores is through clathrate models, as clathrate-like IR features have been identified in interstellar ices,[85] and the presence of different H_2O-clathrate encapsulated species in Earth's[86] and Titan's atmospheres.[87]

Interestingly, even for amorphized systems, ice water molecules tend to form clathrate-like cages.[23] However, to the best of our knowledge, no theoretical works addressing iCOMs formation using clathrate atomistic models are available, while those focusing on the clathrate-molecule interactions are scarce.[23,88] A way to account for the "pore stabilizing effects" is by using the "polarizable continuum model" (PCM).[89,90] PCM is a computationally cheap technique in which solvation effects are described with a continuous dielectric constant ε (the value of liquid water, 78.5, is usually used to simulate solid water[91–93]). Reactive compounds are immersed within the continuum dielectric medium (Figure 3E). However, as solvent molecules are not explicitly considered, specific ice-molecule interactions are omitted. Although this can partly be solved by introducing a "first hydration sphere" of explicit water molecules within the PCM cavity,[94] using a reduced number of water molecules without geometrical constraints can convert the initial pore into a surface due to aggregation phenomena between water molecules.[23]

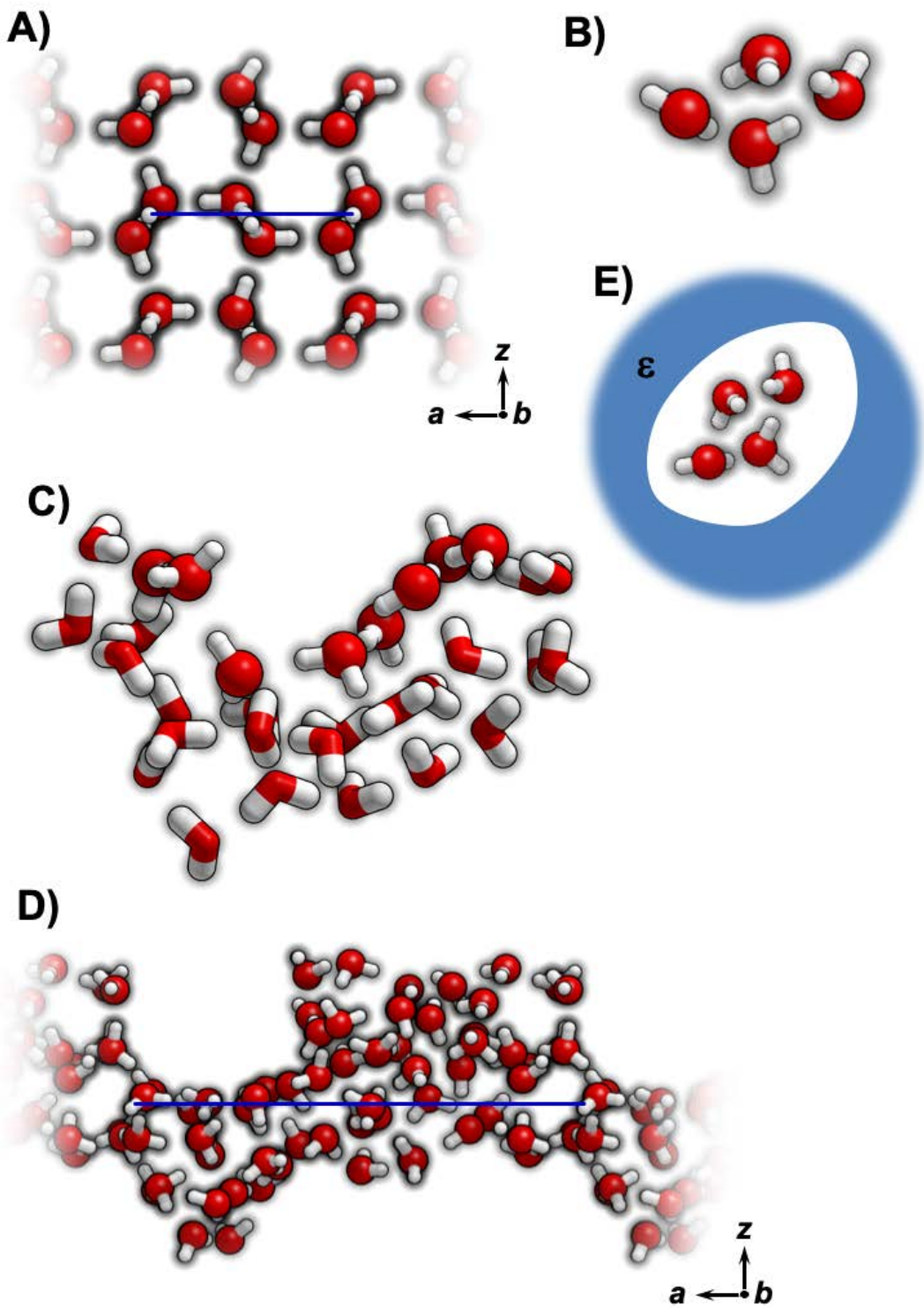

Figure 3. Different strategies to model water ice surfaces: A) Side view of a crystalline 2D-periodic slab model; B) Minimal cluster of 4 waters; C) ONIOM approach for a 33 H_2O cluster: molecules as balls represent the "high level", those as stick the "low level". D) Side view of an amorphous 2D-periodic slab model. E) PCM approach for a 4 H_2O cluster (blue background represents the continuum dielectric ε). For A) and C), ***a*** and ***b*** are the periodic vectors and ***z*** is the non-periodic direction (the ***a*** vector is represented in blue). H-bonds among water molecules are not represented. Colour legend: oxygen in red, hydrogen in white.

3 Computational chemistry works for iCOMs formation

3.1 Formaldehyde (H_2CO) and methanol (CH_3OH) formation

Formaldehyde (H_2CO) and methanol (CH_3OH) are among the few molecules that have been widely detected as components of the icy mantles.[20] From the point of view of iCOMs formation, these two compounds are very important because they are the precursors of more complex species. For instance, their dissociation leads to the formation of HCO·, CH_3O· and CH_2OH· radicals, which can trigger reactions forming iCOMs.

Surface formation of H_2CO and CH_3OH, firstly postulated[95] and then confirmed experimentally,[14,96] takes place through successive hydrogenation of CO, which was previously accreted onto dust grains (see Scheme 1, horizontal path). However, these reactions present competitive processes (represented by the vertical paths), which can make less efficiency H_2CO and CH_3OH formation.

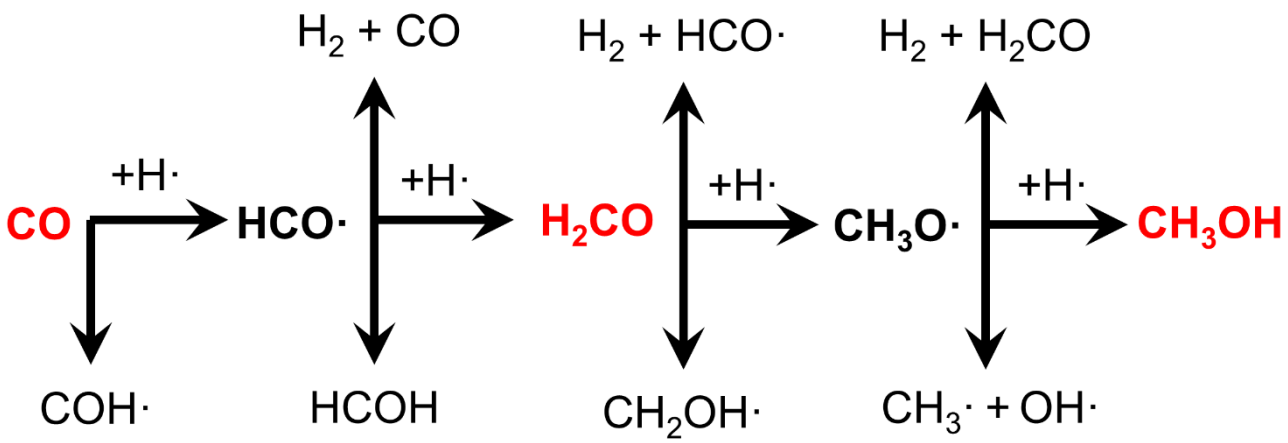

Scheme 1. Formation of formaldehyde (H_2CO) and methanol (CH_3OH) from successive H·-additions to carbon monoxide (CO, horizontal path). Vertical paths refer to competitive channels. Adapted from Ref. 97.

David E. Woon computed the PESs of the first (CO + H· → HCO·) and third (H_2CO + H· → CH_3O·) hydrogenation in the presence of $(H_2O)_n$ clusters (n = 0-4 and 12). For $0 \leq n \leq 4$, post-Hartee-Fock calculations were performed, which were complemented with the PCM solvation approach.[97] Calculated energy barriers varied from 17-70 kJ mol^{-1}, depending on the QM method, n, and PCM application or not. Author concluded that water molecules did not possess a specific

catalytic role in the reactions, probably playing and indirect role (*e.g.*, third body), and opening the possibility that tunneling effects could be important for their occurrence.

More recently, Rimola *et al*.[98] simulated the same reactions in gas phase and in the presence of ice surfaces made up by 3, 18 and 32 H_2O molecules at the BHLPY DFT level. Authors indicated that both reactions presented exceedingly high energy barriers (≈9-14 kJ mol^{-1}) to occur at 10-20 K. Accordingly, tunneling effects were advocated for the occurrence of the reactions. Despite this, authors underlined a catalytic role of water ice since on the ice the energy barriers were slightly lower than in gas phase. Such catalytic effects were associated with bond polarizing effects caused by the interaction of CO and H_2CO with H_2O surface ice molecules, *i.e.*, the C–O bonds became weakened upon interaction, making the C atom more prone to be hydrogenated. Similar results were also found by Goumans *et al*.[99,100] when the reactions occurred on hydroxylated silica surfaces. Here, the C–O bond polarization was induced by the surface Si–OH groups.

Finally, Woon identified an alternative "on-ice" synthetic route for CH_3OH.[101] In this work, it was found that interaction of CH_3^+ with H_2O ice led first to the formation of $CH_3OH_2^+$ (*i.e.*, protonated methanol) and then to the release of the extra proton to the ice to finally form CH_3OH, *i.e.*, $CH_3^+ + (H_2O)_n \rightarrow CH_3OH_2^+ + (H_2O)_{(n-1)} \rightarrow CH_3OH + H_3O^+ + (H_2O)_{(n-2)}$ (see Figure 4). All these processes were found to be barrierless, *i.e.*, they occurred spontaneously during the geometry optimization. Despite the novelty of the path, authors highlighted its dependence on the CH_3^+ interstellar abundance, a controversial aspect since direct observation of CH_3^+ is difficult due to transition symmetry rules so tentative detections are complemented with its CH_2D^+ isotopolog.[102,103]

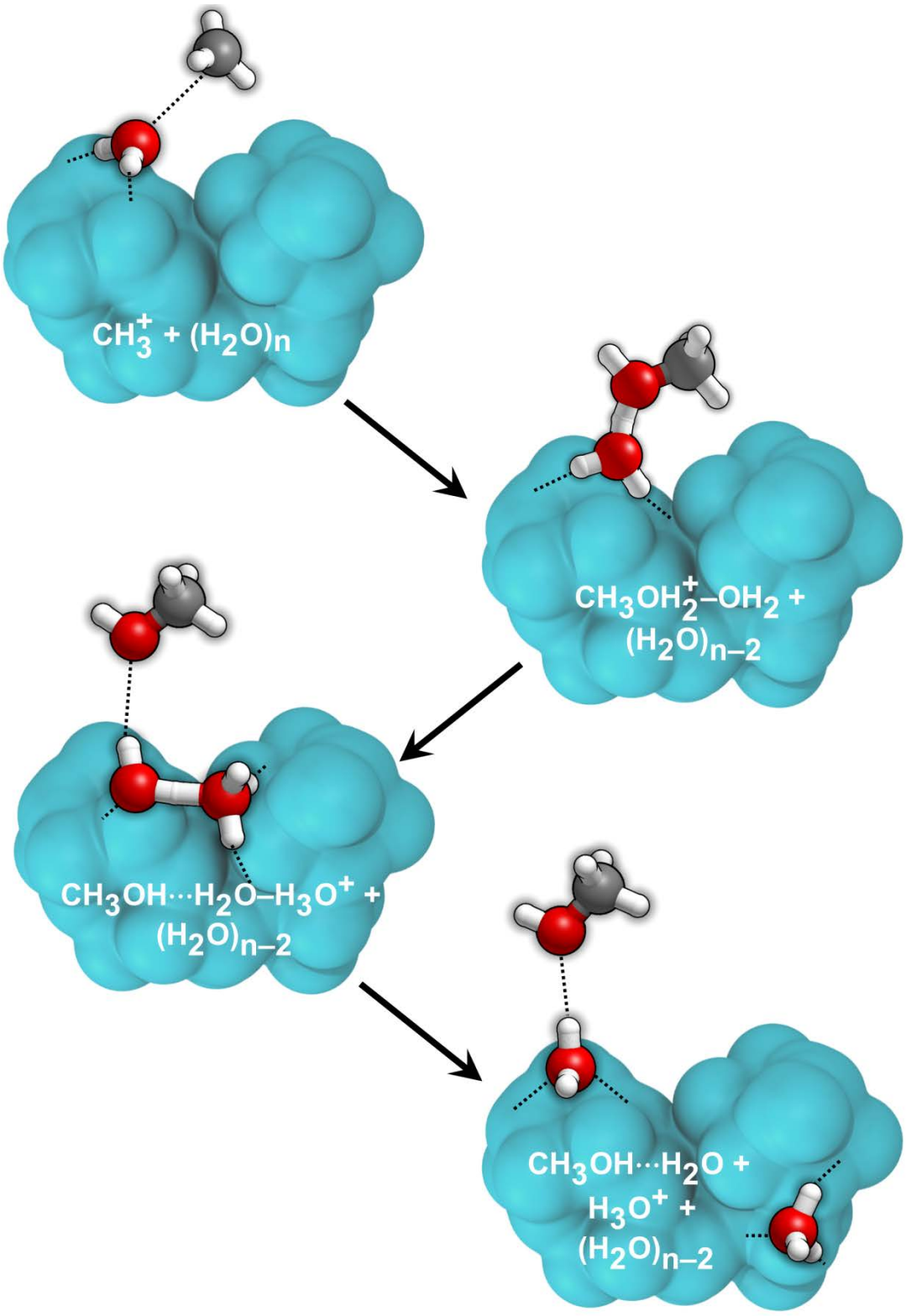

Figure 4. Schematic representation of CH_3OH formation from CH_3^+. Some H_2O molecules are explicitly shown, while the rest are rendered in light blue. Adapted from Ref. 101. Colour legend: oxygen in red, carbon in grey, hydrogen in white.

3.2 Formamide (NH_2CHO) formation

Formamide (NH_2CHO) is one of the molecules that attracted great attention in the last years. It was first detected in 1971 in the massive star forming regions Sgr B2 and in Orion KL1,[7] and since then dedicated observational campaigns have revealed its presence in a variety of star-forming regions, shock sites and protostellar objects,[104–109] as well as comets,[110,111] suggesting a relatively widespread abundance. The astrochemical relevance of formamide arises from manifold aspects: *i*) it is the simplest iCOM containing the four most essential elements for biological systems (*i.e.*, H, C, N and O), *ii*) it is the simplest organic compound containing the amide bond –C(=O)–NH–, the same bond joining amino acids into peptides, and *iii*) there is experimental evidence that it is an effective reactant for the synthesis, in the presence of naturally-occurring minerals and oxides, of precursor biomolecules constituting metabolic and genetic material (see Section 3.8).

Formamide, as other iCOM, is not exempted from the debate whether its formation occurs in the gas phase or on the surfaces of the icy grain mantles. Several theoretical works addressed its gas phase formation through diverse ion-molecule reactions[32,112] and the bimolecular reaction of $H_2CO + NH_2\cdot \rightarrow NH_2CHO + H\cdot$.[27,28] On the ice mantles, its formation has also been addressed by several authors.

Song and Kästner studied the HNCO hydrogenation (*i.e.*, $H\cdot + HNCO \rightarrow NH_2CO\cdot$) on an amorphous water ice cluster model at an hybrid QM/MM theory level.[64] The second hydrogenation was considered to be barrierless, involving a radical-radical reaction. This synthetic route was studied in view of the linear correlation between NH_2CHO and HNCO abundance in different sources.[106] On the ice surfaces, calculated energy barrier adopting an Eley-Rideal mechanism was found to be 4 kJ mol^{-1} lower than in gas phase (31.8 and 36.2 kJ mol^{-1} respectively) due to bond polarizing effects exerted by the ice (similar to hydrogenation of CO and H_2CO, see above[98]). However, tunneling rate constants obtained with the instanton theory were found to be low at the low ISM temperatures, due to a tunneling inefficiency caused by the broad energy barrier width.

These results were in agreement with the inefficient hydrogenation of HNCO ices found experimentally.[113]

Another reaction channel investigated theoretically is the $NH_2\cdot$ + HCO· → NH_2CHO radical-radical coupling on a $(H_2O)_{33}$ cluster model at BHLYP DFT theory level.[114] This "simple" radical coupling followed the usual scheme proposed for iCOMs formation in several astrochemical models,[11,115] and tested experimentally.[116] Results indicated that the actual biradical system (*i.e.*, the two radicals adsorbed on the ice surface with opposite spin states) was stable, precisely because of the interaction with the surface, and that the coupling had an energy barrier of 3 kJ mol^{-1}. However, it was also found that, when the two radicals are properly oriented, a direct H·-transfer from HCO· to $NH_2\cdot$ leading to CO + NH_3 occurred in a barrierless way. H·-transfers of this kind were also observed in acetaldehyde (CH_3CHO) formation HCO· + $CH_3\cdot$ by Enrique-Romero *et al.*:[117] in this case, CH_3CHO formation competed with CO + CH_4 formation, pointing out that reactivity between radicals not always leads to iCOMs formation.

In the same work of Rimola *et al.*,[114] two additional synthetic paths were investigated: reaction of one H_2O molecule of the ice with either HCN or CN·. The first path (*i.e.*, H_2O + HCN → NH_2CHO) was found to have very large energy barriers (167 kJ mol^{-1}), and therefore unfeasible in ISM. The second one (*i.e.*, H_2O + CN· → NH_2CO), however, was found to be energetically favorable due to two aspects: *i*) the high reactivity of the CN· radical, and *ii*) water ice acts as a catalyst by lowering the energy barrier. Indeed, here we present one of the most important aspects of water in the reactions of iCOMs formation, *i.e.* its capability to act as a hydrogen-transfer assistant, with hydrogen having a proton (H^+) character. Upon this role, water molecules belonging to the ice exchange H^+, *i.e.*, they receive one H^+ releasing at the same time another one, helping the transfer process. This role of H^+-transfer assistant can be shared by different water molecules, thus establishing a H^+ relay mechanism. Such a behavior allows both the occurrence of H^+-transfers through a chain of well-connected water molecules and the reduction of the geometrical strains in

TS structures with respect to the gas phase, hence stabilizing them and lowering the energy barriers of the associated H^+-transfer process. As an example, the TS structures for the HNCOH· → NH_2CO· isomerization for water ice acting as H^+-transfer assistant and in gas phase are reported in Figure 5A and B, respectively: the strongly geometrical-strained four-member ring in the gas phase becomes a low strained eight-member ring when three water molecules are present. The final step leading to the formation of the actual NH_2CHO from NH_2CO· was proved to occur via either H·-addition (barrierless) or *via* H·-abstraction of a H_2O ice molecule, in which kinetic results indicated a fast-overall process ($k \sim 10^{-9}$ s^{-1}).

Finally, Bredehöft *et al.*[118] studied – by combining experiments and theory – the synthesis of NH_2CHO under electron exposure of NH_3:CO ice mixtures. Experiments detected NH_2CHO formation and calculations provided a molecular interpretation of these findings (only considering the reactive species, namely, without considering the rest of the ice components). The mechanistic key point was the formation of a transient radical anion NH_3^-·, which triggered the following multi-step reaction: *i*) formation of NH_2· and H^- (barrierless), *ii*) reaction of NH_2· + CO → NH_2CO· (barrierless), and *iii*) reaction of NH_2CO· + NH_3 → NH_2CHO + NH_2·, in which the excess energy provided by the electron attachment was advocated to help overcoming the high energy barrier (≈65 kJ mol^{-1}).

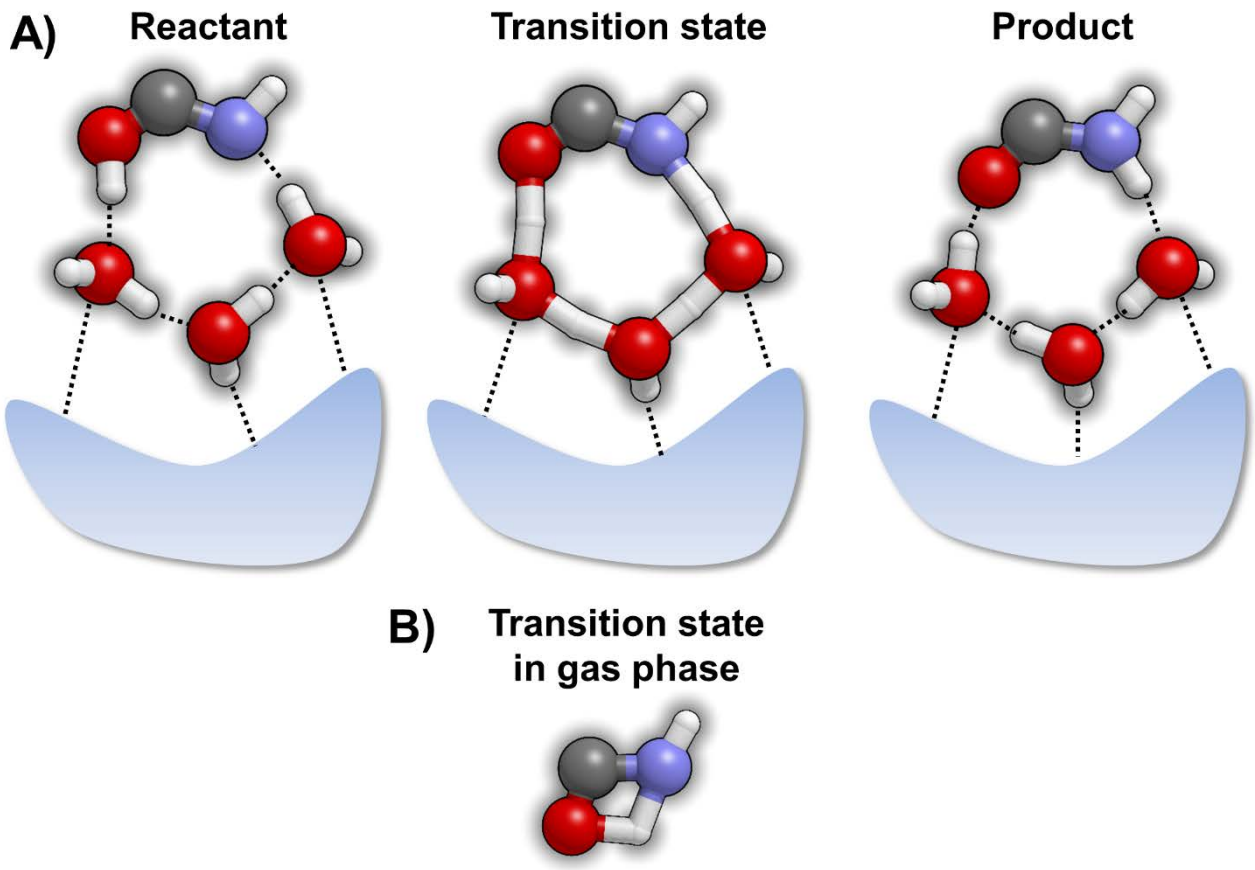

Figure 5. A) Schematic representation of the role of water ice acting as H^+-transfer assistant. In this case, three water molecules are helping the transfer adopting a relay mechanism for the HNCOH· → NH_2CO· isomerization occurring in the CN· + H_2O → NH_2CO· reaction.[114] B) Transition state structure for the HNCOH· → NH_2CO· isomerization in gas phase. Colour legend: oxygen in red, carbon in grey, hydrogen in white.

3.3 Acidic species

3.3.1 Formation HCOOH (and related species) and its reactivity

Woon studied the OH·-addition to CO forming the *trans*-COOH· radical, whose dehydrogenation led to the formation of CO_2, *i.e.*, CO + OH· → *trans*-COOH· → CO_2 + H·.[119] Formation of *trans*-COOH was found to be more favorable than CO_2 in PCM (energy barriers ≈13 and ≈40 kJ mol^{-1}, respectively). In the same work, it was shown that the radical-radical coupling between *trans*-COOH· and CH_2NH_2· yielded glycine formation in a barrierless fashion.

Woon also investigated the formation of HCOOH and CO_2 from the precursors of HCO^+ and "OH^+ + CO", respectively, in a similar way to CH_3OH formation from CH_3^+ (see Section 3.1),[101] *i.e.*:

$$HCO^+ + (H_2O)_n \rightarrow HCOOH_2^+ + (H_2O)_{(n-1)} \rightarrow HCOOH + H_3O^+ + (H_2O)_{(n-2)}$$

$$OH^+ + CO + (H_2O)_n \rightarrow COOH^+ + (H_2O)_n \rightarrow CO_2 + H_3O^+ + (H_2O)_{(n-1)}$$

These processes were identified to occur spontaneously during the geometry optimizations when HCO^+ and "OH^+ + CO" interacted with water molecules of the ice models.

Rimola *et al.*[120] studied the CO + OH· → COOH· reaction on a cage-like $(H_2O)_8$-derivative cluster as water ice surface model. The OH· reactant was initially formed by processing of the $(H_2O)_8$ cluster (see Figure 6), *i.e.*, photolytic removal of one H atom, leading to the formation of a radical neutral cluster (RN path in Figure 6), and one electron removal, leading to the formation of a radical cation cluster (RC path in Figure 6) showing both OH· and H_3O^+. Reaction of these OH· species with CO to form COOH· (Figure 6, last steps) were computed at BHLYP level providing relatively low energy barriers (14 and 12 kJ mol^{-1}, respectively).

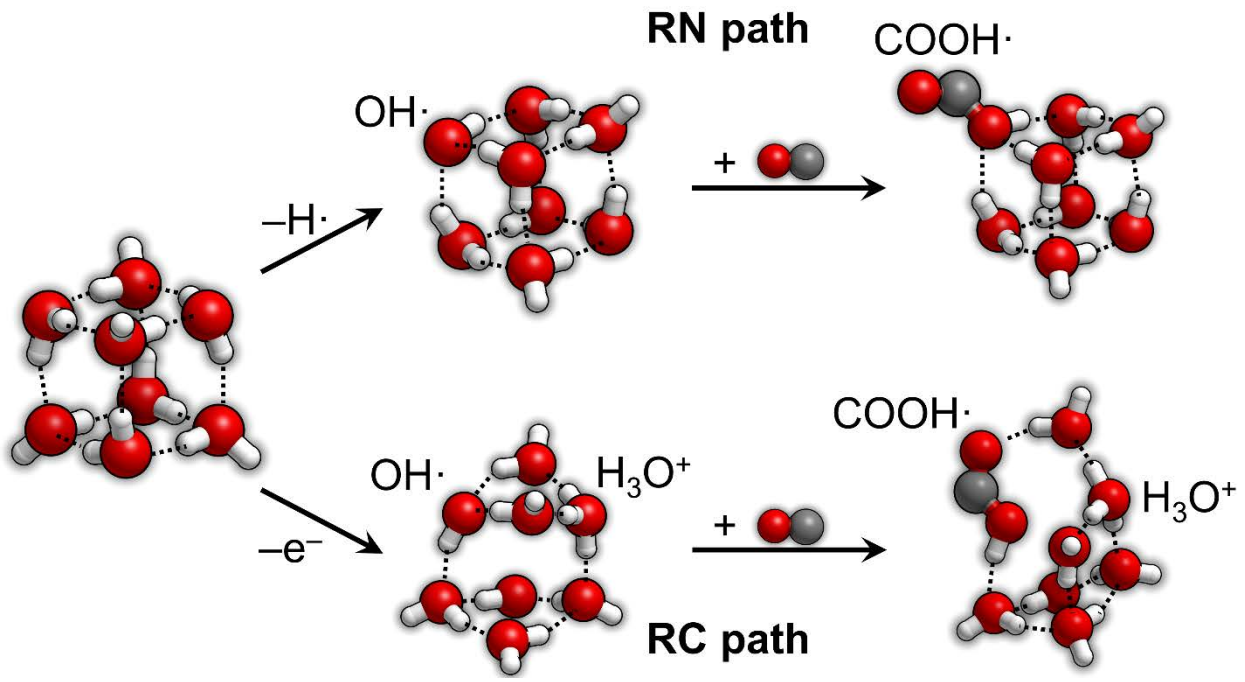

Figure 6. Schematic representation of the formation of COOH· from CO + OH· reaction for the RN and RC paths (see text). OH· comes from the processing of a $(H_2O)_8$ cluster. Adapted from Ref. 120. Colour legend: oxygen in red, hydrogen in white, carbon in grey.

In relation to the HCOOH reactivity, Woon studied the amination of HCOOH in the presence of 0, 1 and 2 H_2O molecules at MP2 level and adopting PCM.[91] Reaction of HCOOH with NH_3 led first

to $NH_2CH_2(OH)_2$ (*i.e.*, hydrated formamide), which eventually dehydrated to give NH_2CHO. In the same work, direct formation of glycine through reaction of HCOOH with CH_2=NH (methanimine) was also investigated. Examined reactions showed large energy barriers, the lowest one being 49 kJ mol^{-1} for the formation of $NH_2CH_2(OH)_2$ in presence of two explicit water molecules, while direct glycine formation showed a very high energy barrier (406 kJ mol^{-1}). Generally, PCM solvation effects lowered the energy barriers by about 5-45 kJ mol^{-1}, while the largest energy decreases were observed when water molecules acted as H^+-transfer assistants (about 80 kJ mol^{-1}, at the most).

Park and Woon focused on the protonation of NH_3 from HCOOH in the presence of explicit waters (2-7, 9, 14, 15 molecules) at B3LYP.[121] The purpose of this work was, rather investigating the reactivity, to reproduce the IR features of the $HCOO^-/NH_4^+$ solid ion pair. In the presence of at least 3 H_2O molecules, H^+-transfer was found to be barrierless. Using "large" (*i.e.*, 7, 9, 14 and 15) H_2O clusters, simulated vibrational features reproduced fairly well the observed ones.[121]

Finally, Kayi *et al*. found that CO_2 and methylamine (CH_3NH_2) on $(H_2O)_n$ ($0 \leq n \leq 20$ clusters) formed the $CH_3NH_2^+/CO_2^-$ ion pair as a result of a charge transfer from CH_3NH_2 to CO_2.[122] It was identified that water favored the charge transfer and the ion pair stabilization.

3.3.2 Reactivity of other acidic species: HOCN/HNCO, HCN/HNC and CH_3COOH

Park and Woon dealt with the deprotonation of cyanic (HOCN) and isocyanic (HNCO) acids reacting with NH_3 with the purpose to: *i*) simulate the reactive processes,[123] and *ii*) check if the "XCN" interstellar band could correspond to one of the resulting species.[124] Different approaches were employed to simulate the water environments, *i.e.*, PCM, small water clusters calculated at full QM methods, and large water clusters calculated with the ONIOM strategy. The main conclusions of these works were that water-assisted deprotonation of both cyanic and isocyanic acid was barrierless in water environments, forming the OCN^-/NH_4^+ ion pair, and that this pair reproduced reasonably well the observationally IR features of the "XCN" band, suggesting OCN^- as a good

candidate carrier. It was also shown that both HOCN and HNCO spontaneously deprotonated even in absence of NH_3, thus forming an OCN^-/H_3O^+ ion pair.

Both hydrogen cyanide (HCN) and isocyanide (HNC) have been observed in the ISM,[125,126] which can be interconverted by the HCN ↔ HNC isomerization. There are essentially two works dealing with this isomerization in water environments. Garderbien and Sevin investigated the reaction in the presence of $(H_2O)_n$ (n = 1-4) clusters at CCSD(T) level.[127] HCN → HNC conversion was found to be thermodynamically disfavoured, the HCN/$(H_2O)_n$ complexes being about 50 kJ mol^{-1} more stable than the HNC/$(H_2O)_n$ ones. Additionally, calculated energy barriers were 178, 124, 96 and 80 kJ mol^{-1} for 1, 2, 3 and 4 H_2O acting as H^+-transfer catalysts, respectively. In the second work, Koch *et al*. investigated the HNC → HCN transformation at B3LYP combining the presence of 3 + 4 water molecules (representing the first + second hydration spheres) with PCM.[94] Authors identified a progressive energy barrier decrease when adding successively solvation effects (*i.e.*, first hydration sphere, the second one, and PCM), reaching the lowest free energy barrier of 11 kJ mol^{-1} at 50 K (all solvation effects accounted for), leading to a half-life time of 714 s. The discrepancies between this two works can be definitely assigned to different adopted models and methods.

Finally, Woon investigated the protonation of NH_3 with acetic acid (CH_3COOH) and HCN/HNC in presence of $(H_2O)_n$ (n = 2-6) clusters at B3LYP and MP2 levels.[128] For all the considered processes, protonation of NH_3 *via* water-assisted mechanisms became barrierless when at least the $(H_2O)_3$ cluster was considered.

3.4 Aminoalcohols formation

Aminoalcohols are organic compounds containing both the alcohol (–OH) group and the amino groups, this latter being primary (–NH_2), secondary (–NH) or tertiary (–N).

Addition of NH_3 to H_2CO yields the formation of aminomethanol (NH_2CH_2OH), the simplest aminoalcohol. However, this process in water environments has methylenglycol ($HOCH_2OH$) formation as a competitive channel (see Scheme 2). In both cases, reactions proceed through a nucleophilic attack of NH_3/H_2O to the C atom of H_2CO followed by a proton transfer to the O atom of the aldehyde C=O group.

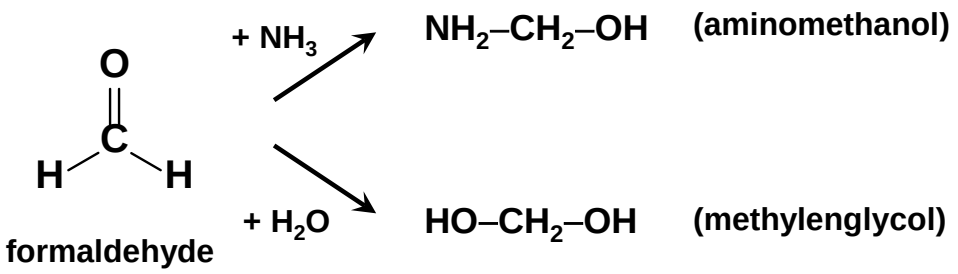

Scheme 2. Formation of aminomethanol and methylenglycol by addition of NH_3 and H_2O, respectively, to formaldehyde.

In a seminal work, Woon investigated these two reactions, alongside polymerization of H_2CO as a possible by-side process, in the presence of explicit water molecules and the PCM solvation model at MP2 level.[129] NH_2CH_2OH formation was found to be the process with the lowest energy barrier (2.5 kJ mol^{-1}) in detriment of $HOCH_2OH$ and H_2CO-polymer formations (energy barriers of 13 and 300 kJ mol^{-1}, respectively). The same author published another article dealing with the formation of more complex aminoalcohols by successive reaction of H_2CO with aminoalcohols formed in previous steps, as well as polyoxymethylenamine H-(-OCH_2-)$_n$-NH_2 (POM-NH_2), an aminoalcohol polymeric form (Scheme 3).[130] Results indicated that, regardless of the catalytic effects exerted by the PCM environment and the presence of explicit water molecules, these reactions were not likely to occur in interstellar conditions because of their relatively high energy barrier, with values ranging from 20 to 140 kJ mol^{-1}.

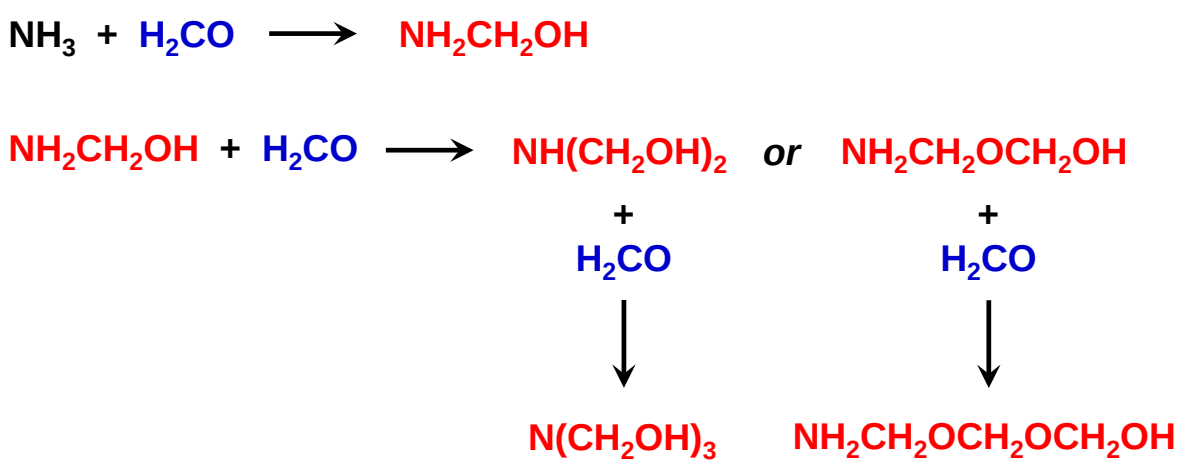

Scheme 3. Successive reactivity of formaldehyde (in blue) with aminoalcohols (in red).

Courmier *et al.*[131] refined Woon's calculations[129] for the NH_2CH_2OH formation in the presence of $(H_2O)_n$ (n = 0-3) explicit molecules at CCSD(T) level. Figure 7A shows the initial structure of the reaction, in which NH_3 and H_2CO interacted with a the $(H_2O)_3$ cluster adopting a pentamer-like configuration in the way to maximize the H-bond interactions. All calculated energy barriers were found to be systematically higher by about 15 kJ mol^{-1} than those obtained by Woon.[129] Nevertheless, the role of water acting as H^+-transfer assistant was clearly shown, with energy barriers of 150, 75 and 50 kJ mol^{-1} for n = 0, 1 and 2, respectively. For n = 3 the energy barrier was found to slightly increase compared with n = 2.

In a more recent work, Rimola *et al.*[132] simulated the same reaction of NH_2CH_2OH formation on a water ice surface modelled by 18 H_2O molecules at B3LYP level. Figure 7B shows the initial structure of the reaction. An energy barrier of 40 kJ mol^{-1} was computed, disagreeing by some amount with that of 60 kJ mol^{-1} found by Courmier *et al.*[131]. The reasons of such a difference arise from both the different theory levels and the different water ice models, where in the Rimola's one[132] more water molecules were implicated in the H^+ transfer-assistance and its surroundings, inferring stabilizing effects.

All these mentioned works based the NH_2CH_2OH formation reaction on a concerted mechanism, in which the nucleophilic attack and the proton-transfer occurred synchronically. However, Chen and

Woon found that when the H_2CO and NH_3 reactants were well-encaged, fully surrounded by water ice molecules, the C–N coupling took place spontaneously forming the NH_3^+–CH_2O^- zwitterionic compound (see Figure 7C).[133] Zwitterions are neutral species bearing localized charges which are stabilized by water solvent effects. In this case, 4 H_2O molecules are enough to induce the barrierless formation of NH_3^+–CH_2O^- and its stabilization. Subsequent proton-transfer (assisted by the water molecules) leading to final NH_2CH_2OH was computed to have an energy barrier of 13 kJ mol^{-1} (B3LYP level and PCM). Similar zwitterion spontaneous formation was also observed more recently by Riffet *et al*.,[93] where the $H_2CO/NH_3/(H_2O)_n$ (n = 0-4) complexes were studied within the PCM model at G3B3 DFT theory level. In this work, with only 3 H_2O molecules NH_3^+–CH_2O^- formation was already observed. Calculated energy barrier of the water-assisted H^+-transfer was 20 kJ mol^{-1} (for n = 4), 7 kJ mol^{-1} higher than that calculated by Chen and Woon.[133] Differences arise from both the level of theory and the configuration of the water clusters, in which the Riffet's ones resemble more to a water ice surface (see Figure 7D). For the sake of completeness, Riffet *et al*. also investigated the formation of NH_3^+–CH_2OH (protonated aminomethanol) by reaction of H_2CO with the ammonium cation (NH_4^+).[93] Computed barriers were found to be significantly higher compared with the neutral processes, *e.g.*, 125 kJ mol^{-1} for n = 4.

As mentioned above, NH_2CH_2OH formation in water ice media can have a competitive channel, *i.e.*, $HOCH_2OH$ formation. This synthetic route was studied by Duvernay *et al*. on a water ice surface model of 33 H_2O molecules ate B3LYP level.[134] Results indicated that pure reaction of $H_2CO + H_2O \rightarrow HOCH_2OH$ (in which the reacting H_2O belonged to the ice) occurred *via* formation of a transient H_3O^+/OH^- pair, in which OH^- performed the nucleophilic attack. This process was calculated to have an energy barrier of ≈70 kJ mol^{-1}. However, the presence of NH_3 in the ice catalyzed the reaction because of the easier formation of the NH_4^+ /OH^- ion pair as intermediate (energy barrier ≈8 kJ mol^{-1}), followed by the OH^- nucleophilic attack (energy barrier ≈20 kJ mol^{-1}) forming deprotonated $HOCH_2O^-$ methylenglycol. Protonation of $HOCH_2O^-$ was carried out by the

NH_4^+ (energy barrier ≈39 kJ mol^{-1}, the highest one). By comparing the energetics for NH_2CH_2OH and $HOCH_2OH$ formations, it is clear that the former process is more favorable. However, one has to keep in mind that for NH_2CH_2OH formation, NH_3 has to be in stoichiometric quantities with H_2CO (it is the reactant), while for $HOCH_2OH$ traces are enough to act as catalyst. Accordingly, occurrence of one reaction or the other will strongly depend on the initial amount of NH_3.

Formation of aminoalcohols from acetaldehyde (CH_3CHO) and acetone [$(CH_3)_2CO$] proceeds in a similar way as for aminomethanol, *i.e.*, CH_3CHO and $(CH_3)_2CO$ react with NH_3 to give $NH_2CH(CH_3)OH$ (1-aminoethanol) and $NH_2C(CH_3)_2OH$ (2-amino-2-propanol), respectively, following the same "nucleophilic attack + proton-transfer" mechanism. These two reactions were simulated by Fresneau *et al*. on different amorphous water-dominated dirty ice mantles at B3LYP-D3 level,[135,136] and by Chen & Woon[133] in an already mentioned work (see above). For all cases, water acting as H^+-transfer assistant was found to be essential to lower the energy barriers compared with the gas phase processes. In the Fresneau's works, both processes adopted a stepwise mechanism, in which the first step involved the N–C coupling forming the NH_3^+-$CH(CH_3)O^-$ and NH_3^+-$C(CH_3)_2O^-$ zwitterions followed by H^+-transfer. As for the NH_2CH_2OH case, in the Chen & Woon work, zwitterion formations were spontaneous, at variance with respect to the Fresneau's ones. Differences can be explained by the different H_2O ice models: in the Fresneau's model, both the reactive species interacting with water and the same water molecules of the cluster were largely geometrically constrained due to the H-bond network (hence representing more realistic ice surface properties), while in the Chen and Woon's ones, reactants were fully surrounded by H_2O molecules and/or the clusters were geometrically exceedingly flexible, hence overestimating the stability of the zwitterion induced by water. The highest calculated energy barriers for $NH_2CH(CH_3)OH$ and $NH_2C(CH_3)_2OH$ formations were ≈34 and ≈26 kJ mol^{-1}, respectively, in the Fresneau's works and about 12-13 kJ mol^{-1} in the work by Chen & Woon,[133] the energetic differences being due to the different ice models (as explained above).

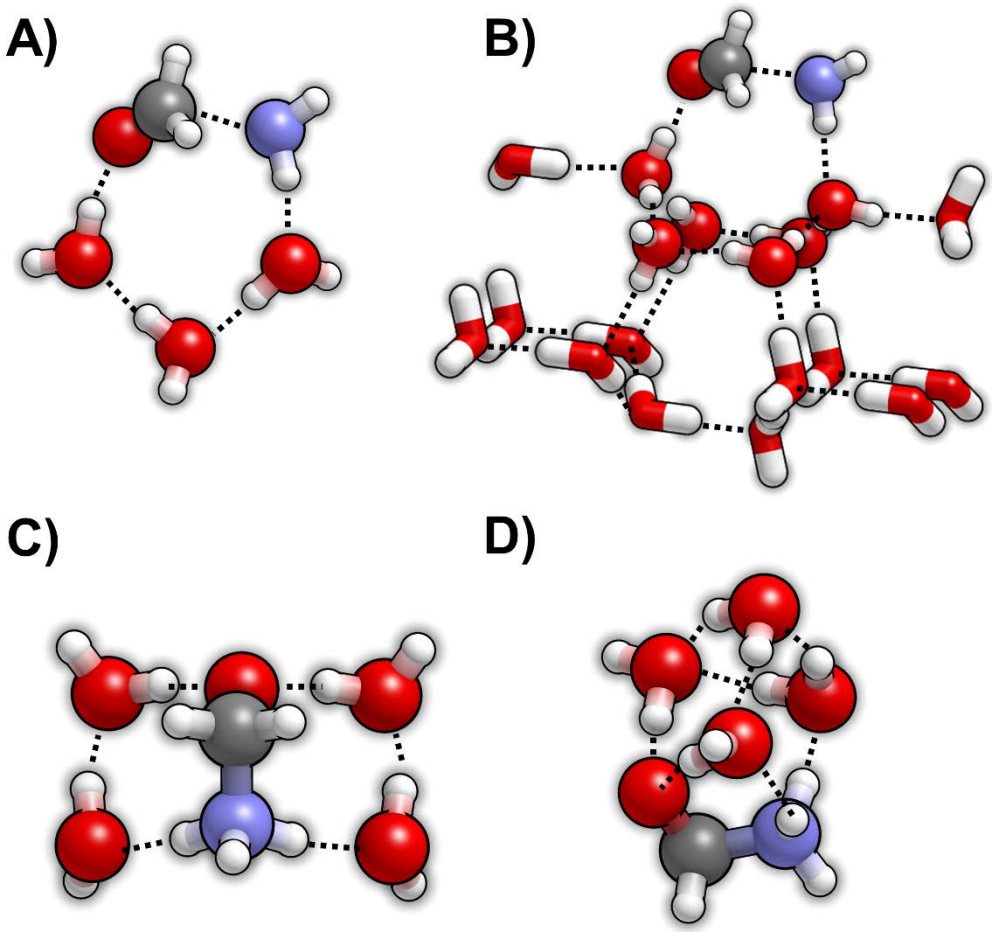

Figure 7. Representative initial structures for the formation of NH_2CH_2OH from reaction of H_2CO with NH_3: A) with a $(H_2O)_3$ cluster model;[131] B) with a $(H_2O)_{18}$ cluster model as water ice surface (atoms involved in the H^+-transfer assistance were highlighted as balls);[132] C) with a $(H_2O)_4$ cluster model;[133] and D) with a $(H_2O)_4$ cluster model.[93] In these two later systems, the NH_3^+–CH_2O^- zwitterion was spontaneously formed. Colour legend: oxygen in red, carbon in grey, nitrogen in blue and hydrogen in white.

3.5 Methanimine (CH_2=NH) formation and reactivity

The aforementioned works of Rimola *et al.*[132] and Riffet *et al.*[93] also dealt with the dehydration of aminomethanol to form methanimine (CH_2=NH). In the former work,[132] the –OH and –NH_2 groups of aminomethanol acted as H-bond acceptor and donor groups, respectively, thus enabling the dehydration reaction through a water-assisted H^+-transfer mechanism. Despite the catalytic behavior of water, the reaction presented an energy barrier of ≈90 kJ mol^{-1}. In the second work,[93] the same reaction was also studied using diverse water cluster models, presenting energy barriers of 100-150 kJ mol^{-1}. In this work, moreover, a charged mechanism was also studied involving the

dehydration of $HOCH_2NH_3^+$ (previously formed by reaction of NH_4^+ with H_2CO). This path presented relatively lower energy barriers, between 70-90 kJ mol^{-1}.

Hydrogenation of HCN to form CH_2=NH was studied by Woon following the reactions shown in Scheme 4.[119] The PESs of each step were characterised in absence of explicit water molecules but using the PCM model at QCISD(T) level. Results indicated that for the first H·-addition, CH_2N· formation was more favorable than HCNH· (energy barriers of 30.5 *vs* 53.6 kJ mol^{-1}, respectively), while the second one was considered to be barrierless.

Scheme 4. Hydrogenation of HCN leading to the formation of methanimine (in red). Compounds in blue are the two possible radical intermediates.

In relation to CH_2=NH reactivity, its hydration (leading to NH_2CH_2OH) by reaction with one water molecule and a second one acting as H^+-assistant was calculated to have an energy barrier of 119 kJ mol^{-1} in PCM conditions, while its amination to give diaminomethane ($CH_2(NH_2)_2$) catalysed by one H_2O molecule in PCM had an energy barrier of 83 kJ mol^{-1}.[91] Reactivity of CH_2=NH with HCN giving aminoacetonitrile (NH_2CH_2CN) has also been studied. Since acetonitriles are a family of iCOMs extensively investigated theoretically, formation of these compounds is reviewed in a new section presented below.

3.6 Acetonitrile-derivatives formation

Acetonitrile is the compound with chemical formula CH_3CN. The most relevant feature is the nitrile C≡N group. In this section, theoretical studies related to the formation of acetonitrile-derivatives on interstellar ice mantles are reviewed.

3.6.1 Hydroxyacetonitrile ($HOCH_2CN$) and hydroxyacetoisonitrile ($HOCH_2NC$) formation

$HOCH_2CN$ and $HOCH_2NC$ are two hydroxylated acetonitrile compounds that can be formed by reaction of H_2CO with HCN and HNC, respectively. Although the reactants have widely been detected in the ISM,[125,126,137] only $HOCH_2CN$ has been detected very recently.[138] Woon examined these two reactions, as well as the subsequent reactivity of these compounds with a second H_2CO molecule (see Scheme 5), all of them in the presence of $(H_2O)_n$ (n = 0-2) clusters at the MP2 level in PCM.[139] In the same work, the HCN + H_2O → NH=CHOH and HCN + NH_3 → $NH{=}CHNH_2$ reactions were also investigated. Results indicated that reactivity with HNC presented lower energy barriers than with HCN (*e.g.*, 66 and 109 kJ mol^{-1} for the formation of $HOCH_2CN$ from HNC and of $HOCH_2NC$ from HCN on $(H_2O)_2$ in PCM, respectively, see Scheme 5). Moreover, reaction energies were found to be negative in the former case, while slightly positive in the latter one. However, as shown above, HNC is more unstable than HCN (about 50 kJ mol^{-1}) and hence the difference in the energetic features of these reactions.

$$\mathrm{HCN} + \mathrm{H_2CO} \longrightarrow \mathrm{HOCH_2NC}$$

$$\mathrm{HNC} + \mathrm{H_2CO} \longrightarrow \mathrm{HOCH_2CN}$$

$$\mathrm{HOCH_2CN} + \mathrm{H_2CO} \longrightarrow \mathrm{HOCH_2OCH_2CN}$$

$$\mathrm{HOCH_2NC} + \mathrm{H_2CO} \longrightarrow \mathrm{HOCH_2OCH_2NC}$$

Scheme 5. Reactions simulated by Woon in the presence of small H_2O clusters.[139] Nitrile species are in red, while isonitriles in green.

More recently, Rimola and coworkers studied the $HOCH_2CN$ formation by reaction of HCN with H_2CO on a water ice model of 33 H_2O molecules at B3LYP-D3 level.[140] Results indicated that this reaction was activated by a proton-transfer of the HCN to the H_2O ice, forming the H_3O^+/CN^- ion pair, in which CN^- was the responsible of the nucleophilic attack to the C atom of the C=O group (see Figure 8). The resulting intermediate was $^-OCH_2CN$ (deprotonated hydroxyacetonitrile), the protonation of which was performed by recovering the proton initially transferred to the ice. Here, the role of the ice was not as H^+-transfer assistant but allowing the generation of the CN^- anion. The first step presented the highest energy barrier, ≈54 kJ mol^{-1}, which is significantly lower to that calculated by Woon.[139] Interestingly, authors also explored the formation of $HOCH_2OCH_2CN$ by reaction of the $^-OCH_2CN$ intermediate (formed in the second step) with a second H_2CO molecule. The coupling between the C atom of H_2CO with the charged O atom of $^-OCH_2CN$ presented a very low energy barrier (2.5 kJ mol^{-1}), indicating the feasibility of the process.

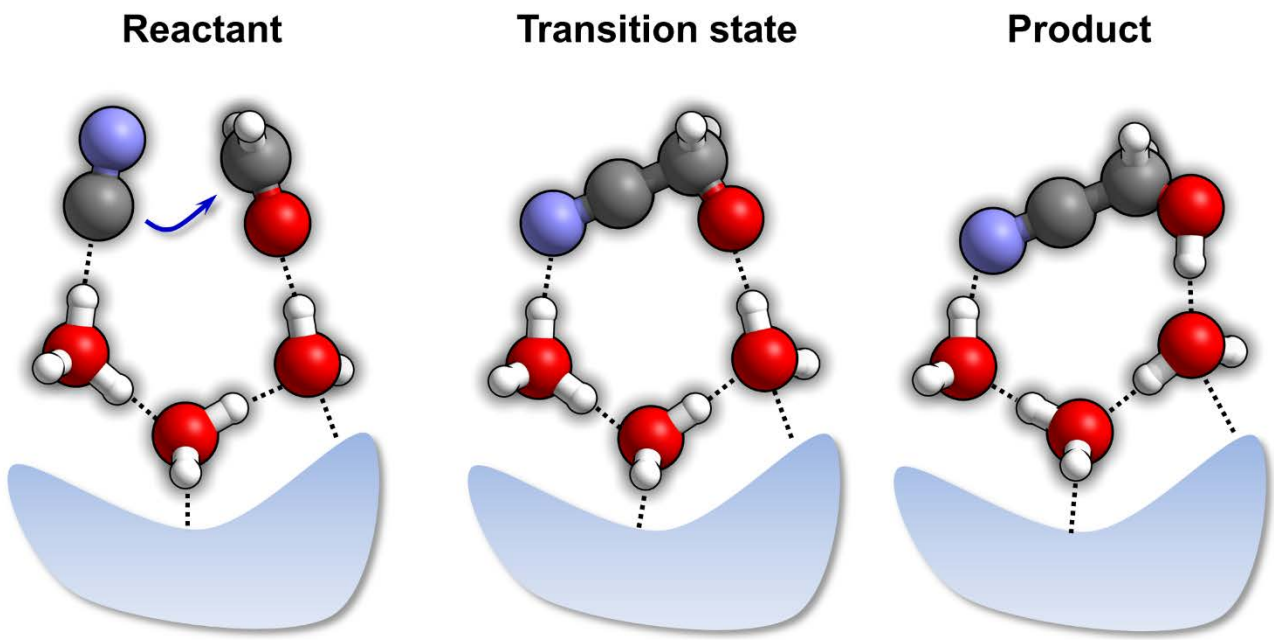

Figure 8. Schematic representation of the $HOCH_2CN$ formation on a water ice surface through previous formation of the H_3O^+/CN^- ion pair. The blue arrow indicates the nucleophilic attack of the C atom of CN^- anion to carbonyl group of H_2CO. Adapted from Ref. 140.

Rimola and coworkers also investigated the reactivity of HCN with CH_3CHO and $(CH_3)_2CO$ leading to the formation of $HOCH(CH_3)CN$ and $HOC(CH_3)_2CN$, respectively, in these cases

adopting diverse dirty ice surface model clusters.[135,141] Simulated reaction mechanisms were the same as for the H_2CO case, presenting similar energy barriers (50-54 kJ mol^{-1}). Interestingly, calculations also indicated that the presence of traces of NH_3 in the ice favoured the formation of the CN^- anion because of the larger stability of the NH_4^+/CN^- pair than the H_3O^+/CN^- one, which was reflected by a significant decrease of the energy barriers (about 30-35 kJ mol^{-1}).

3.6.2 Aminoacetonitrile (NH_2CH_2CN) and aminoacetoisonitrile (NH_2CH_2NC)

NH_2CH_2CN and NH_2CH_2NC can be formed by reaction of CH_2=NH with HCN and HNC, respectively. Among these two nitriles, only NH_2CH_2CN has been detected in Sgr B2(N).[142] Computational formation of these two compounds was first investigated by Woon at MP2 level in PCM conditions.[91] The reaction mechanisms adopted are summarized in Scheme 6, in which NH_2CH_2CN formed *via* a two-step process, *i.e.*, reaction of CH_2=NH with HCN to give NH_2CH_2NC which then isomerized into NH_2CH_2CN. Nevertheless, direct formation of NH_2CH_2CN can occur by the addition of HNC to CH_2=NH. The two-step mechanism was computed to have energy barriers of 96 and 110 kJ mol^{-1}, while the direct one 40.5 kJ mol^{-1}.

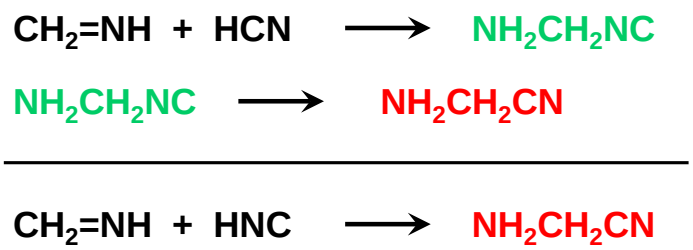

Scheme 6. Formation of NH_2CH_2CN from CH_2=NH studied by Woon.[91] Two-step mechanism (first addition of HCN to CH_2=NH to give NH_2CH_2NC and subsequent isomerization to NH_2CH_2CN, top) vs direct reaction with HNC (bottom). Nitriles in red, isonitriles in green.

In a more recent work, Koch *et al*. examined the NH_2CH_2CN formation by reaction of CH_2=NH with HCN in the gas phase, in the presence of $(H_2O)_n$ (n = 1-3) clusters, and in the presence of 2 water molecules acting as proton transfer assistants plus 12 water molecules acting as ice spectators, all of them at B3LYP level.[92] Authors considered two different mechanisms: a direct one, in which

NH_2CH_2CN was formed by reaction of CH_2=NH with HNC (previous HCN → HNC isomerization), and an indirect one, in which NH_2CH_2NC was first formed, which then isomerized into NH_2CH_2CN. The free energy profiles at 50 K for the gas phase reactions, in the presence of a $(H_2O)_2$ cluster, and with the "2+12" H_2O ice model are shown in Figure 9A and B for the direct and indirect mechanisms, respectively, in which the gas phase optimized geometries are also shown. The catalytic role of water is evident from these energy profiles, since energy barriers decrease successively when the water ice model is improved. The indirect path was found to be more favourable, with free energy barriers of 26 kJ mol^{-1}, while the direct one presented a free energy barrier of 46 kJ mol^{-1} due to the initial HCN → HNC isomerization.

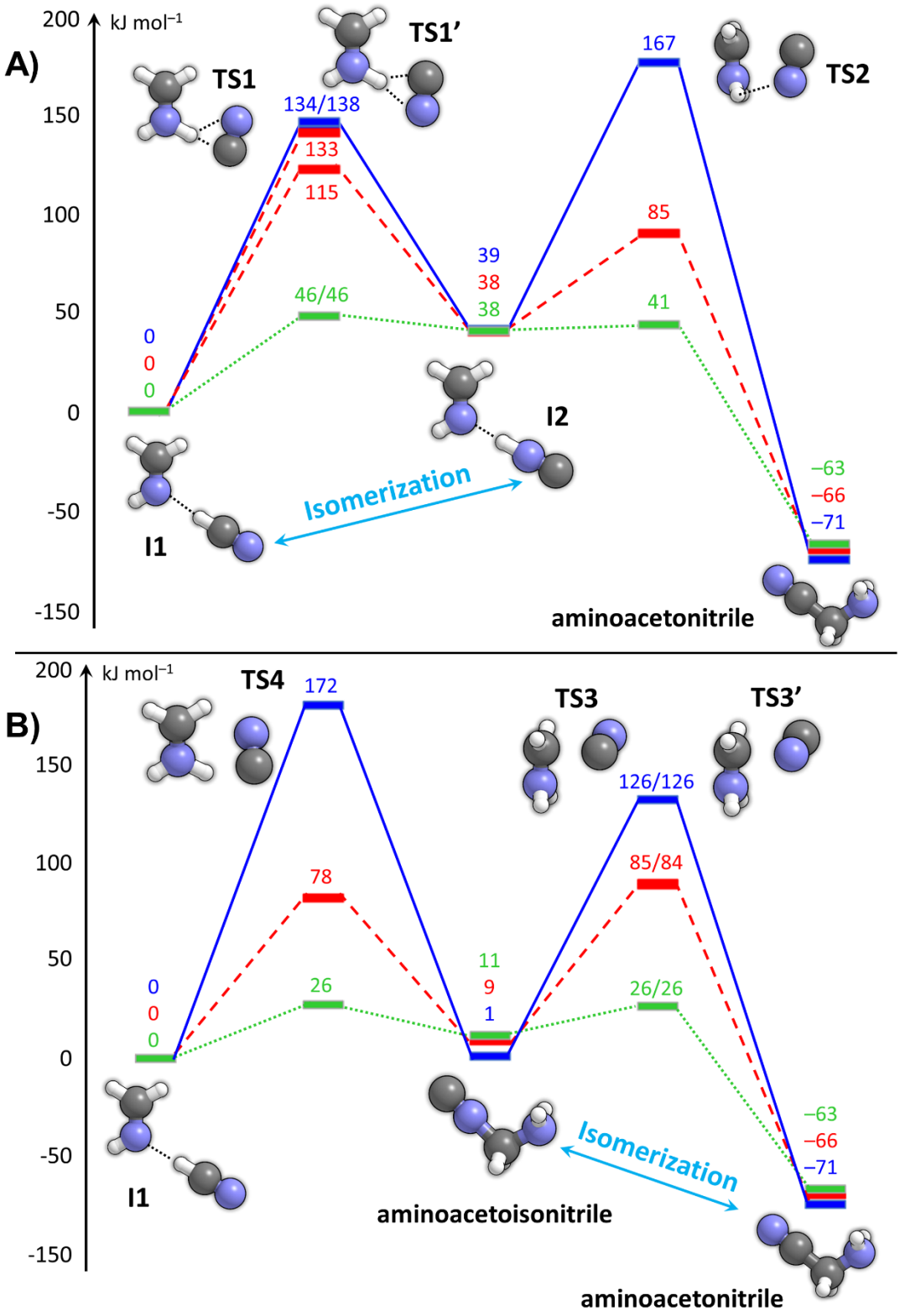

Figure 9. Free energy profiles (in kJ mol^{-1}) at 50 K for the direct (A) and indirect (B) formation of NH_2CH_2CN from CH_2=NH and HCN in gas phase (solid blue lines) in the presence of a $(H_2O)_2$ cluster (dashed red lines) and in the presence of the "2+12" H_2O ice model (dotted green lines). Adapted from the work of Koch *et al.*[92] We keep the same nomenclature of the stationary points of the original work. Optimized gas phase geometries are also shown. Atom color legends: carbon in grey, nitrogen in blue and hydrogen in white.

Finally, Rimola *et al*. also studied NH_2CH_2CN formation on a water ice cluster model of 18 molecules at B3LYP level.[132] They first simulated the direct path, namely, HCN → HNC first and then CH_2=NH + HNC → NH_2CH_2CN, whose energy barriers (adopting water-assisted H^+-transfer mechanisms) were ≈75 and ≈82 kJ mol^{-1}, respectively. In addition, authors also investigated an ionic path. It started first with a proton-transfer from HCN to CH_2=NH (energy barrier of ≈73 kJ mol^{-1}), forming the $CN^-/CH_2NH_2^+$ ion pair, stabilized by interaction with the water ice. Then the CN^- anion performed a nucleophilic attack to the C atom of $CH_2NH_2^+$ yielding final NH_2CH_2CN with an energy barrier of 3 kJ mol^{-1}.

3.7 Glycine formation

Glycine (NH_2CH_2COOH), the simplest amino acid, has been identified in comets[143–145] and its presence in meteorites (among other amino acids) is usual.[146] The traditional route for the synthesis of amino acids is the Strecker synthesis.[147] It involves different steps, some of them already commented above: *i*) reaction of an aldehyde (RCHO, with R being a lateral chain) with ammonia to give the corresponding aminoalcohol, *i.e.*, RCHO + NH_3 → $NH_2CH(R)OH$; *ii*) dehydration of the aminoalcohol to give the corresponding imine, *i.e.*, $NH_2CH(R)OH$ → CH(R)=NH + H_2O; *iii*) reaction of the imine with HCN to give the corresponding aminonitrile, *i.e.*, CH(R)=NH + HCN → $NH_2CH(R)CN$, and *iv*) acidic hydrolysis of the nitrile group which is converted firstly into an amide (–$CONH_2$) and finally to an acid (–COOH) group, *i.e.*, $NH_2CH(R)CN$ + $2H_2O$ → $NH_2CH(R)COOH$ + NH_3. These steps are schematically represented in Figure 10 for the particular case of glycine formation, in which the aldehyde is H_2CO (R=H).

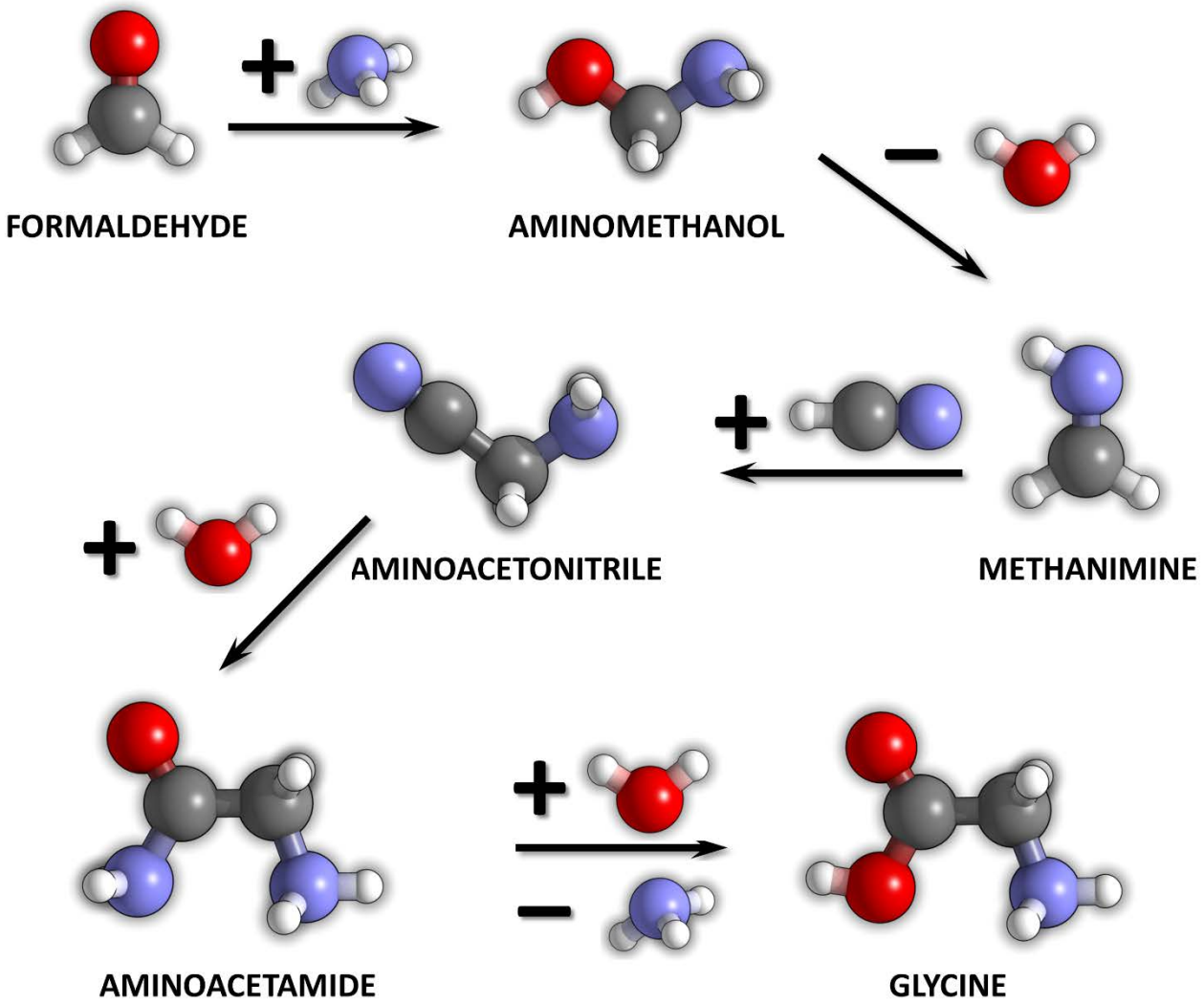

Figure 10 Different steps of the Strecker synthesis of glycine from formaldehyde. Colour code: oxygen in red, carbon in black, nitrogen in blue and hydrogen in white.

Interestingly, all the Strecker initial species (H_2CO, NH_3, HCN, H_2O) are relatively abundant interstellar molecules and Rimola *et al*. simulated this synthesis on a water ice surface model of 18 H_2O molecules in PCM.[132] The first three steps, namely, formation of aminomethanol, methanimine and aminoacetonitrile, have been commented above (Sections 3.4, 3.5 and 3.6.2, respectively), thus, here we focus on the final step, the hydrolysis of the aminoacetonitrile, which involves the successive nucleophilic attack of two H_2O molecules on the C atom of the nitrile. Calculated energy barriers were found to be the highest ones of the overall process (159 and 163 kJ mol^{-1}), a fact which led the authors to conclude that the entire Strecker synthesis is unlikely at the cryogenic

temperatures, advocating for external energy inputs such as UV radiation and cosmic rays to be overcome.

These findings stimulated the same authors to investigate an alternative route for glycine formation accounting for these energy inputs.[120] In Section 3.3.1 we reported formation of COOH· on processed water ice clusters (see Figure 6). That work was within the context of glycine formation, in which the next step after COOH· formation was its reactivity with CH_2=NH. On the RN cluster, such a coupling, leading to formation of the $NHCH_2COOH\cdot$ radical, was computed to have an energy barrier of 50 kJ mol^{-1}. On the RC cluster, authors identified an almost barrierless proton-transfer from the H_3O^+ species to CH_2=NH, and the formed $CH_2{=}NH_2^+$ cation coupled to COOH· through a lower energy barrier of 26 kJ mol^{-1}, to form the $NH_2CH_2COOH\cdot^+$ radical cation. Due to the enhanced acidity of the CH_2 group of this radical cation, authors simulated that one H atom could be transferred to the ice (energy barrier of ≈30 kJ mol^{-1}) so that the $NH_2CHCOOH\cdot$ radical was ready to react with other radicals, to form different amino acids (*e.g.*, H· or $CH_3\cdot$ to give glycine or alanine, respectively).

Alternative paths beyond the Strecker synthesis have also been computed. In a couple of works, Nhlabatsi *et al*. investigated formation of interstellar glycine adopting two different channels based on the CH_2=NH reactivity: *i*) $CH_2{=}NH + CO + H_2O \rightarrow NH_2CH_2COOH$,[148] and *ii*) $CH_2{=}NH + CO_2 + H_2 \rightarrow NH_2CH_2COOH$.[149] For both reactions, authors found a concerted mechanism in which all the components reacted synchronically (Figure 11). Despite the elegance of these mechanisms, the energy barriers were found to be 172 kJ mol^{-1} (142 kJ mol^{-1} if assisted by an additional H_2O molecule) and 303 kJ mol^{-1}. For these two reactions, authors also investigated a stepwise mechanism initiated by formation of the $C(OH)_2$ carbene (via $CO + H_2O$ and $CO_2 + H_2$ reactions, respectively), which upon reaction with CH_2=NH led to glycine. Although this later step was found to have a relatively low energy barrier (38 kJ mol^{-1}), the processes were hindered by the high energy barriers of the carbene formation (270 and 300 kJ mol^{-1}, respectively).

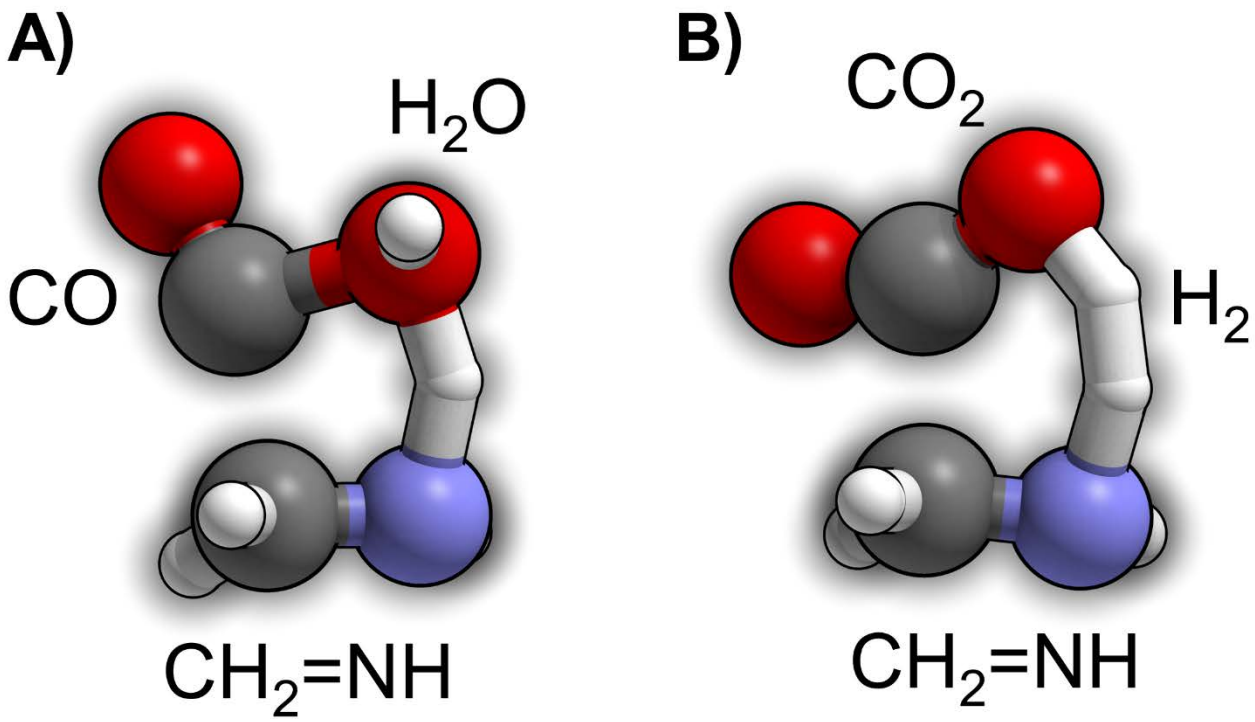

Figure 11 Transition states for the concerted formation of glycine from CH_2=NH + CO + H_2O (A, Ref. 148) and CH_2=NH + CO_2 and H_2 (B, Ref. 149). Colour code: oxygen in red, carbon in black, nitrogen in blue and hydrogen in white.

Lee and Choe investigated the formation of glycine from HCN oligomers reacting with H_2O.[150] It was found that the HCN trimer, $NH_2CH(CN)_2$, reacted with one H_2O molecule to form $NH_2CH(CN)CONH_2$, and that water additions to this compound led to glycine formation through different paths, which were catalyzed by one water molecule assisting the H^+-transfers. It was found the former reaction exhibited an energy barrier of 106 kJ mol^{-1} and that among the different investigated paths, the one involving $NH_2CH(CN)CONH_2$ + $2H_2O$ → glycine + HNCO + NH_3 was the most energetically favorable, with an overall energy barrier of 169 kJ mol^{-1}.

Finally, Kayanuma *et al*. investigated formation of glycine *via* a hydantoin mechanism.[151] Hydantoin (2,4-imidazolidinedione) is an important precursor yielding glycine upon hydrolysis an it can be formed by CO_2 addition to aminoacetonitrile (see Scheme 7). Hydantoin has been identified in Murchison and Yamato-791198 meteorites.[152,153] The reaction was simulated by the authors in the presence of two H_2O molecules acting as proton-transfer catalysts. Reactivity of aminoacetonitrile with CO_2 leading to hydantoin involved several steps, the highest energy barrier

being 111 kJ mol^{-1}. Hydantoin hydrolysis, performed by two H_2O molecules and accompanied by NH_3 and CO_2 elimination, exhibited intrinsic energy barriers between 176-255 kJ mol^{-1}. Authors pointed out that these energy barriers were too high to be overcome at cryogenic conditions even considering interstellar time-scales (10^6 years).

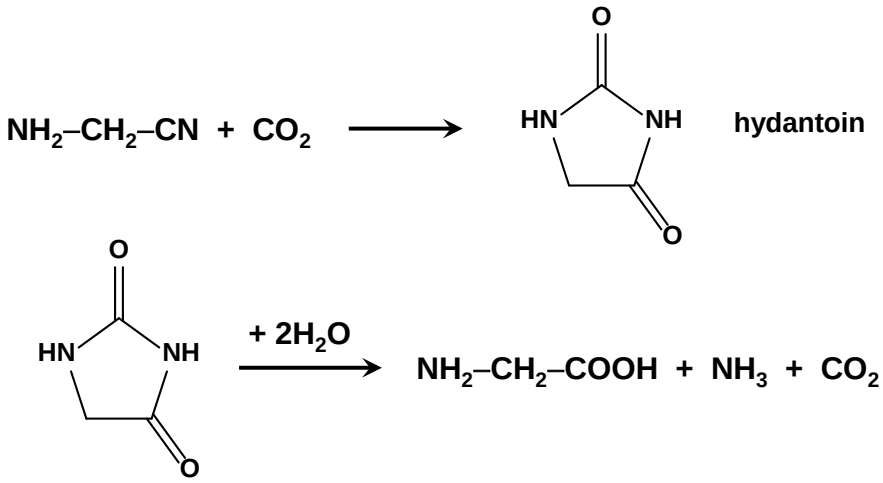

Scheme 7. Formation of hydantoin by reaction of aminoacetonitrile NH_2CH_2CN with CO_2 (above) and its hydrolysis to give Gly (below).

Another interesting amino acid precursor is the hexamethylenetetramine (1,3,5,7-tetraazatricyclo-[3.3.1]-decane, $C_6H_{12}N_4$, HMT), a fourth-cycled molecule whose hydrolysis seem to form amino acids. Its solid-phase formation under astrophysical conditions has been simulated from reactivity of H_2CO and NH_3 in HCOOH-rich ices by Vinogradoff *et al*. in 2012.[154] The reaction involved first formation of NH_2CH_2OH followed by water elimination to form CH_2=NH and then reactivity between several CH_2=NH molecules to form HMT. The identified mechanism consisted of a complex process with eight steps, in which the coexistence of CH_2=NH and CH_2=NH^+ (this latter forming an ion pair with $HCOO^-$) was crucial to activate the HMT formation by CH_2=NH additions. In addition to elucidating a plausible reactions mechanism, theoretical calculations also served to identify an intermediate species detected experimentally. The highest computed barrier is for the NH_2CH_2OH dehydration to CH_2=NH, for which authors compute a thermal barrier at 70 K equal to 53.3 kJ mol^{-1}.

3.8 Nucleobases

Origin of nucleobases identified in meteorites is not well known. It seems, however, that formamide (NH_2CHO) is an essential precursor towards their formation. Several experimental works showed a selective reactivity of NH_2CHO on different mineral surfaces (*e.g.*, montmorillonite, titania, silica, etc.) towards formation of several nucleobases and derivatives.[155–162]

The detailed formation mechanism of nucleobases is a matter of debate. A first paradigm postulates that NH_2CHO dehydrates first into HCN, the polymerization of which (or reaction with NH_2CHO) leads to nucleobase formation. Another one advocates that NH_2CHO polymerizes itself forming nucleobases and relates species (see Figure 12).[163–165]

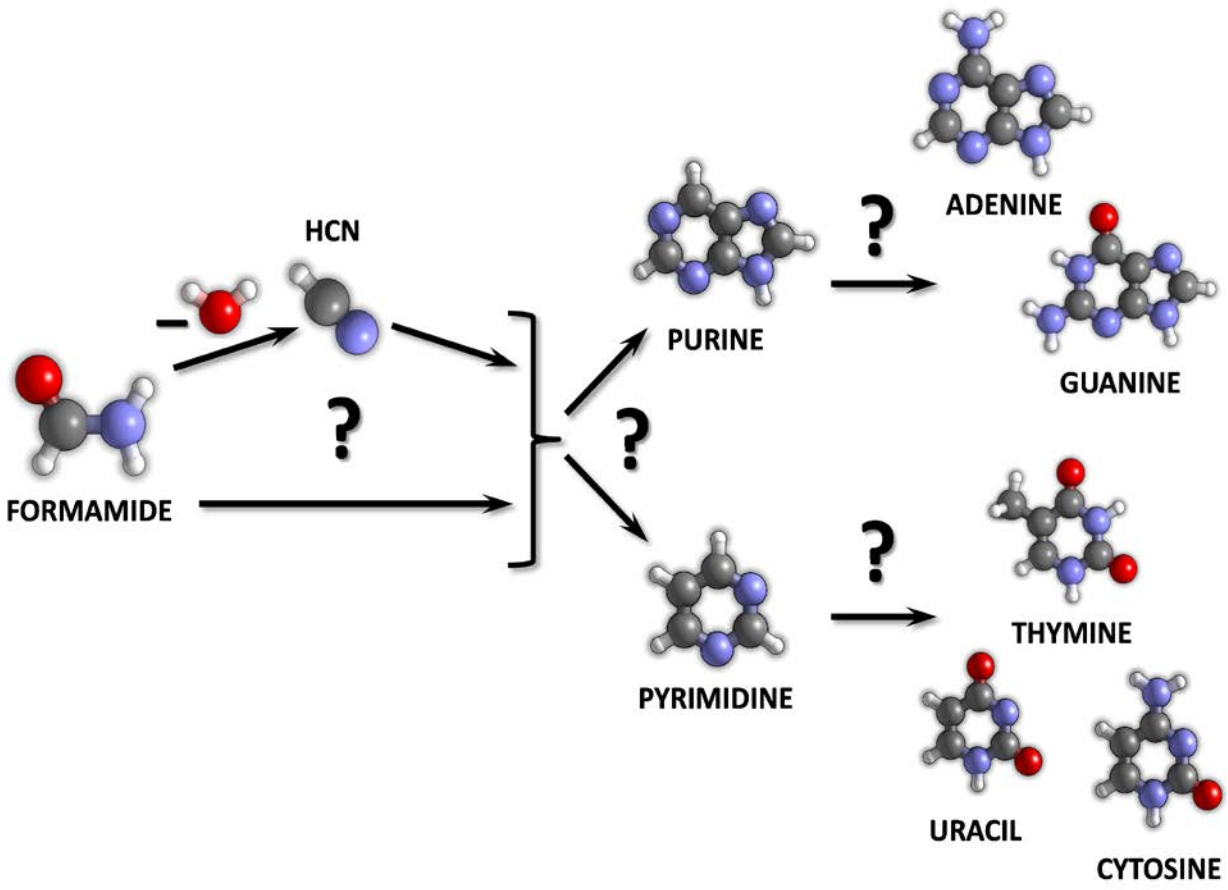

Figure 12. Pyrimidine, purine and nucleobases as products of either formamide decomposition into HCN followed by successive polymerization and reactivity or direct formamide polymerization and reactivity. Colour code: oxygen in red, carbon in black, nitrogen in violet and hydrogen in white.

Detailed mechanisms of nucleobase formation and the role of water in these reactions from an atomistic point of view are very scarce. Nevertheless, few computational works can be found in literature.

As regard the first paradigm, Ngueyn *et al*. have explored dehydration of formamide in presence of 1, 2 and 3 water molecules, at CCSD(T) level of theory.[163] Authors identified two possible routes: *i*) one occurring through the H_2N–C–OH carbene species and forming HNC, and, *ii*) the other occurring via the HN=CH–OH imine species and forming HCN. The latter is kinetically favored since all the energy barriers are lower. In both routes, the role of the water was to favor the H^+-transfers, although barriers are too high in ISM conditions (the lowest one being 130 kJ mol^{-1}). Despite this, in the case HCN to be formed, it was shown it could polymerize towards nucleobases or related species.[163]

Bera *et al*. investigated the formation of uracil (U) considering oxidation of pyrimidine (Py) induced by UV photolysis at B3LYP and MP2 theory levels in absence and presence of a single H_2O molecule.[166] Here, rather than providing full PESs, the thermodynamics of the different mechanisms were investigated (*i.e.* no transition states and kinetic barriers were computed). The first favourable step was the reaction of OH· (assumed to be derived from H_2O photolysis) with Py or its radical cations form, $Py\cdot^+$ (also assumed to be formed by UV effects). Formation of different mono-hydroxylated products were considered since OH· can react with any of the six positions of $Py/Py\cdot^+$. The two most stable ones were 4(3*H*)-pyrimidone and 2(1*H*)-pyrimidone and their tautomeric forms 4-hydroxypyrimidine and 2-hydroxypyrimidine (Scheme 8). The single water molecule was found to help the H^+ abstraction during the OH· addition. A second OH· addition into these two stable products led to the formation of U as di-hydroxylated product (see Figure 12). These reactions were also energetically favoured by the presence of water.[166]

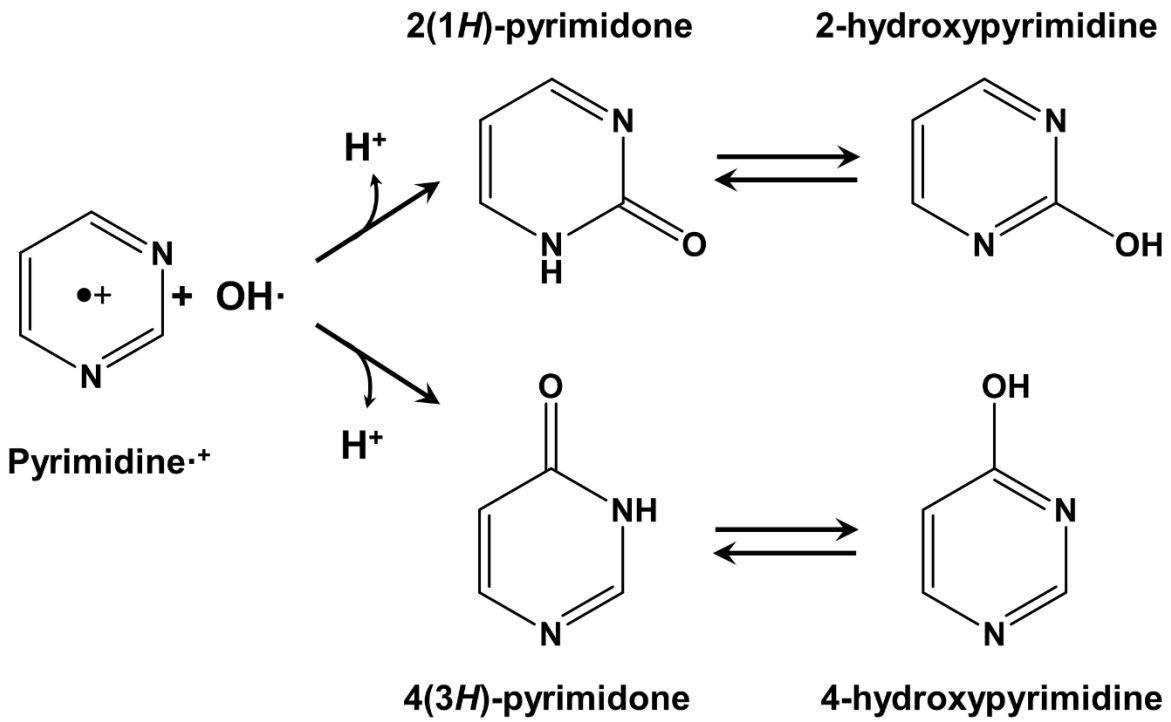

Scheme 8. Formation of mono-hydroxylated products from the OH· addition followed by H^+ elimination to the radical cation of pyrimidine. From Ref. 166.

In a more recent work, the same authors extended the calculations to study the formation of thymine (T, see Figure 12).[167] In this case, different radical routes were considered, combining two OH· additions with one CH_3· addition. It was found that the formation of T from Py through two successive OH· additions followed by a CH_3· addition was the most thermodynamically favourable path. The presence of an explicit H_2O molecule helped the H^+ abstraction of the intermediate species.

Formation of adenine (A) and guanine (G), from purine (Pu) was also explored by Bera *et al*. adopting the same idea to investigate the thermodynamic stability of different radical addition paths in the absence and presence of one H_2O molecule, in this case at B3LYP level and in PCM.[168] In particular, authors investigated the OH· and NH_2· additions onto the radical cation of Pu (Pu·$^+$). The most stable products identified were 2-hydroxyhypurine and 6-hydroxypurine (hypoxanthine) for OH· addition, while 2-aminopurine and 6-aminopurine (adenine) for NH_2· addition (see Scheme 9). Interestingly, NH_2· addition onto hypoxanthine led to formation of G, while OH· addition to A

formed isoguanine. The role of the explicit water was again to help the H^+ abstractions, while PCM effects induce an additional stabilization of the products of these reactions.

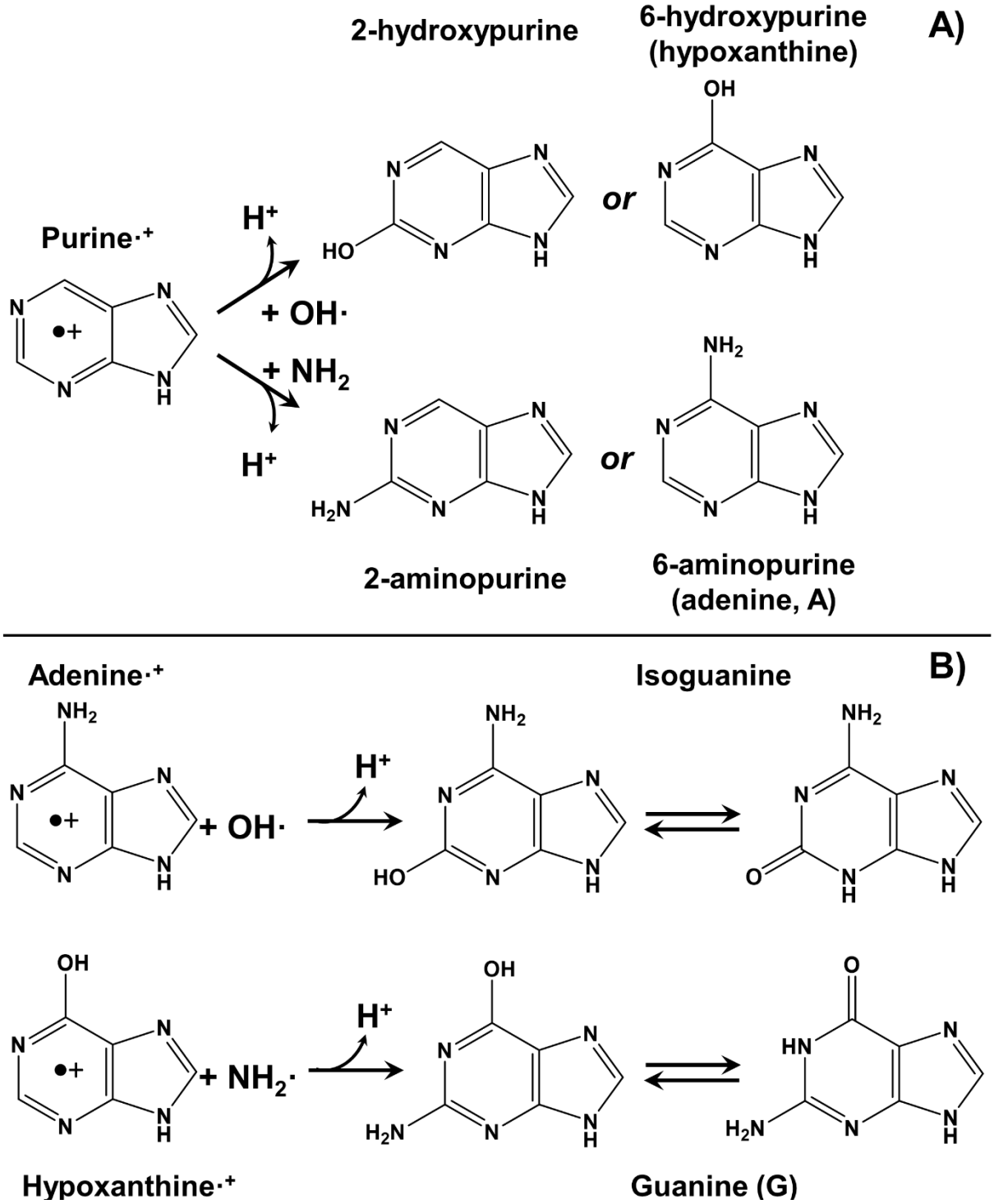

Scheme 9. A) OH· and NH_2· additions followed by H^+ elimination to the radical cation of purine. One of the products is adenine. B) OH· and NH_2· addition followed by H^+ elimination to the radical cations of products formed in A). One of the products is guanine. From Ref. 168.

3.9 iCOMs from meteorite impacts

Cometary ices, similar to the interstellar ones, are predominated by H_2O but also contain other volatile species such as CO_2, NH_3 and CH_3OH.[51] Additionally, recent analysis of dust samples from comet Wild 2 and 67/P showed the presence of glycine in the captured material[145,169] These cometary ices could undergo high energy processes due to impacting with planetary surfaces. High energetic impacts generate strong pressure waves that propagate through the ice mantle, which eventually can ignite complex reactivity. This section reviews few computational works focused on the simulation of the chemistry taking place in an impacting cometary ice.

From a computational point of view, a high-pressure impact can be simulated by adopting multiscale shock-compression simulation technique, which is based on AIMDs in 3D periodic models. In this technique, periodic parameters are forced to shrink within a certain short time and then relaxed, *i.e.*, expanded and cooled down up to thermalization of the systems. Such a procedure was carried out by Goldman and coworkers to investigate the chemistry triggered by high-pressures of a mixture ice with composition of $20H_2O$, $10CH_3OH$, $10NH_3$, 10CO and $10CO_2$ *per* 3D unit cell.[51,52]

In a former study,[51] authors adopted expensive AIMDs introducing shock velocities of 5, 6, 7, 8, 9, 10 km s^{-1} for 5–11 ps (2 ps only for 10 km s^{-1}), corresponding to initial impact pressures of 10, 18, 24, 37, 47 and 59 GPa, and temperatures of 706, 1196, 1590, 2549, 3141 and 4083 K, respectively. After the impact period, systems were decompressed and cooled down (relaxed) for some ps. Authors analyzed the eventual formation of new bonds among the initial reactant mixture. The most interesting finding of this work was the formation of a Gly-related species at 9 km s^{-1} (47 GPa): the high-pressure impact caused the formation of a long C–N-bonded oligomer containing the –NH–CH_2–COOH sequence. In the relaxation phase, such oligomer broke apart forming several C–N-bearing species such as HCN and NH_2–COOH, but the sequence corresponding to Gly remained intact. This molecular complex could eventually react with protonated species to form glycine; for

instance, $^{-}OCO–NH–CH_2–COOH + H_3O^+ / NH_4^+ \rightarrow NH_2–CH_2–COOH + CO_2 + H_2O/NH_3$, with free reaction energies of –101.3/–9.2 kJ mol^{-1}.

An analogous procedure was adopted in a second work,[52] but at Density Functional Tight Binding (DFTB) level, which is a simplified version of standard QM calculations which is close to molecular mechanics in terms of computer resources. With the same initial ice composition of the previous work, shocks at 36, 48, 60 GPa for 100 ps (phase 1), followed by adiabatic expansions (phase 2) and final cooling at 300 K (phase 3) were simulated. In phase 1, several new C–C and C–N bond forming species were identified, the actual composition depending on the given pressure. Some of these transient species decomposed during phase 2. Among survival species, in phase 3, authors identified amino acids precursors as well as aliphatic and aromatic hydrocarbons.

Table 1 Summary of all the reviewed works. Acronyms legend: CO, carbon monoxide; CH_3OH, methanol; H_2CO formaldehyde; HCOOH, formic acid; CO_2^-, carboxylate anion; CO_2, carbon dioxide; FoAm, formamide; HCO·, formyl radical; NH_2·, amino radical; CH_3· methyl radical; CN·, cyanil radical; AM, aminomethanol; MG, methylenglicole; POM, polyoxymethylene; AcAl, acetaldehyde; Ac, acetone; HCN, hydrogen cyanide; HNC, hydrogen isocyanide; Gly, glycine; NH_3, ammonia; NH_4^+, ammonium cation; CH_2=NH, methanimine; CH_3NH_2, methylamine; HOCN, cyanic acid; HNCO, isocyanic acid; CH_3COOH, acetic acid; HAN, hydroxyacetonitrile; HAisoN, hydroxyacetoisonitrile; AAN, aminoacetonitrile; HMT, hexamethylenetetramine; Py, pyrimidine; Pu, purine; U, uracil; A, adenine; G, guanine; T, thymine.

Topic	**Molecules**	**QM Method**	**Ice model**	**Reference**
Hydrogenation of CO to form H_2CO and CH_3OH	CO, H_2CO, CH_3OH	MP2, QCISD, ONIOM	1-4, 12H_2O PCM	97
Hydrogenation of CO to form H_2CO and CH_3OH	CO, H_2CO, CH_3OH	B3LYP, CCSD(T)	3, 18, 32H_2O	98
Hydrogenation of CO to form H_2CO and CH_3OH	CO, H_2CO, CH_3OH	QM/MM	No water: on silica surfaces	99
Hydrogenation of CO to form H_2CO and CH_3OH	CO, H_2CO, CH_3OH	QM/MM	No water: on silica surfaces	100
Formation of CH_3OH, HCOOH and CO_2 through cationic reactions	CH_3OH, FH, CO_2	B3LYP, MP2	4, 17H_2O	101
Hydrogenation of HNCO to form FoAm	HNCO, FoAm	QM/MM	Hemispherical cluster cut from amorphous slab	64
Formation of FoAm from HCO· + NH_2·, HCN + H_2O and CN· + H_2O	HCO·, NH_2·, HCN, CN·, FoAm	BHLYP	33H_2O	114
Formation of AcAl from HCO· + CH_3·	HCO·, CH_3·, AcAl	M06-2X-D3 B3LYP	18, 33H_2O	117
Formation of FoAm from CO + 2NH_3	CO, NH_3, FoAm	B3LYP	No water	118
Hydrogenation of HCN to form CH_2=NH Radical formation of HCOOH and CO_2	HCN, CH_2=NH, HCOOH, CO_2	QCISD, QCISD(T)	PCM	119
Reactions of FH and CH_2=NH with NH_3 Direct formation of Gly from HCOOH + CH_2=NH	HCOOH, CH_2=NH, NH_3, Gly	MP2	1, 2H_2O PCM	91
Formation of NH_4^+/CO_2^- by protonation of NH_3 from HCOOH	HCOOH, NH_3, NH_4^+/CO_2^-	B3LYP	2-7, 9, 14, 15H_2O	121

Formation of a $CH_3NH_2^+/CO_2^-$ ion pair	CH_3NH_2, CO_2, $CH_3NH_2^+/CO_2^-$	B3LYP	nH_2O, $0 \leq n \leq 20$	122
Formation of NH_4^+/OCN^- by protonation of NH_3 from HOCN/HNCO.	HOCN, HNCO, NH_3	B3LYP, ONIOM	2-15H_2O PCM	123
Reproduction of "XCN" interstellar band	HOCN, HNCO, NH_3	B3LYP	2-12H_2O	124
HCN ↔ HNC isomerization	HCN, HNC	MP2, CCSD(T)	1-4H_2O	127
HCN ↔ HNC isomerization	HCN, HNC	B3LYP	Reaction core: 3H_2O Solvation: 12H_2O, PCM	94
Deprotonation of CH_3COOH, HCN, HNC in water ice	CH_3COOH, HCN, HNC	B3LYP, MP2	2-6H_2O	128
Formation of AM from H_2CO + NH_3 Formation of MG from H_2CO + H_2O	H_2CO, AM, MG	MP2	PCM	129
Formation of POM from AM	AM, POM derivatives	MP2	PCM	130
Formation of AM from H_2CO + NH_3	H_2CO, AM	B3LYP, MP2, CCSD(T)	1-3H_2O	131
Reactivity of H_2CO, AcAl and Ac with NH_3	H_2CO, AcAl, Ac, aminated products	B3LYP	2, 4, 9, 12H_2O PCM	133
Two first steps of glycine Strecker's synthesis	H_2CO, AM, CH_2=NH,	B3LYP	1-4H_2O	93
Formation of MG from H_2CO + H_2O (with NH_3 presence)	H_2CO, MG	B3LYP	33H_2O	134
Formation of $H_2NCH(CH_3)OH$ from AcAl + NH_3 Formation of $NCCH(CH_3)OH$ from AcAl + HCN	AcAl, HCN, NH_3	B3LYP-D3	12H_2O	135
Formation of $HOC(CH_3)_2NH_2$ from Ac + NH_3	Ac, NH_3	B3LYP-D3	15H_2O	136
Formation of HAN and HAisoN from H_2CO + HNC/HCN and isomerization	H_2CO, HCN/HNC, HAN, HAisoN	MP2	PCM	139
Formation of HAN, HAisoN and POM-CN from H_2CO + HNC/HCN	H_2CO, HCN, POM-CN	B3LYP	33H_2O	140

Formation of $HOC(CH_3)_2CN$ from Ac + HCN (with NH_3 presence)	Ac, HCN, NH_3	B3LYP-D3	$33H_2O$	141
Formation of AAN from CH_2=NH + HCN/HNC	MI, HCN/HNC, AAN	B3LYP	Reaction core: $3H_2O$ Solvation: $7H_2O$, PCM	92
Glycine Strecker's synthesis	H_2CO, AM, CH_2=NH, AAN, Gly	B3LYP	$18H_2O$	132
Radical formation of Gly from HCOOH and MI	HCOOH, CH_2=NH, Gly	BHLYP	$8H_2O$	120
Formation of Gly from CH_2=NH + CO + H_2O	CH_2=NH, CO	B3LYP and several others	1-$4H_2O$	148
Formation of Gly from CH_2=NH + CO_2 + H_2	CH_2=NH, CO, CO_2, H_2	B3LYP and several others	No water	149
Formation of Gly from $H_2NCH(CN)CONH_2$	$H_2NCH(CN)CONH_2$, Gly	B3LYP, CBS-QB3	$1H_2O$	150
Formation and Gly *via* hydantoin	AAN, hydantoin, Gly	B3LYP	1-$3H_2O$	151
Formation of HMT from reactivity of CH_2=NH	H_2CO, HMT, CH_2=NH, HCOOH, AM, NH_3	B3LYP	NH_3:H2CO:FH mixed clusters but no ice model	154
Dehydration of FoAm to form H_2O + HCN/HNC	FoAm, HCN/HNC	MP2, CCSD(T)	1-$3H_2O$	163
Interaction and dehydration of FoAm on silica surfaces. No kinetic barriers	FoAm	PBE	No water: silica surfaces	170
Radical formation of U from Py. No kinetic barriers	Py, U	B3LYP, MP2	No water	166
Radical formation of T from Py (*via* U). No kinetic barriers	Py, T, U	B3LYP, MP2	No water	167
Formation of A and G from Pu·. No kinetic barriers	Pu, A, G	B3LYP	PCM	168
Formation of iCOMs in impacting cometary ices	H_2O, CH_3OH, NH_3, CO, CO_2	B3LYP	$20H_2O$:$10CH_3OH$:$10NH_3$:10CO:$10CO_2$	51
Formation of iCOMs in impacting cometary ices	H_2O, CH_3OH, NH_3, CO, CO_2	DFTB	$20H_2O$:$10CH_3OH$:$10NH_3$:10CO:$10CO_2$	52

4 Conclusions and future perspectives

In this work, most of the quantum mechanical studies addressing the formation of iCOMs on ice mantles have been reviewed. They are not only focused on standard iCOMs but also to simpler organic compounds as well as those of increased complexity, *i.e.*, formation of H_2CO and CH_3OH, NH_2CHO, acidic organic species (*e.g.*, HCOOH), aminoalcohols, CH_2=NH, acetonitriles, glycine and nucleobases. The different reaction-types yielding their formation have also been revised theoretically: hydrogenations, radical additions, radical-radical couplings, and ion-ion, ion-neutral and neutral-neutral reactions. All the reviewed works, including useful details, are summarized in Table 1.

Since water is the main constituent of interstellar ices, ice mantles were simulated by either explicit water molecules or implicitly with PCM solvation models. It was shown that water exerted from moderate to strong catalytic effects in the reactions. They were particularly important when water molecules were explicitly considered due to their role as H^+-transfer assistants, in which the energy barriers decreased as a consequence of the lower geometrical strains in TS structures than in gas phase. In other cases, water stabilized ion pairs, allowing the occurrence of ion-induced reactions. Despite these catalytic effects, most of the energy barriers were calculated to be significantly high to occur at typical temperatures of MCs (10-20 K) and, accordingly, activation by temperature was in most of the cases claimed.

All the reviewed works have contributed to improve our know-how of the iCOMs formation on ice mantles, by figuring out the processes from a molecular standpoint, providing exclusive structural and energetic features, and helping us to assess their feasibility under interstellar conditions. However, several relevant aspects remain still missing.

One of them deals with the plausibility of the occurrence of water-assisted H^+-transfer processes adopting a relay mechanism on ice surface mantles. To take place, the implicated waters must be connected by H-bond interactions in a suitable way as they can be capable to donate and receive H^+

properly. However, whether this situation is indeed present or not in actual ice mantles and how the structural state and the presence of other ice components can affect this water catalytic property are still open questions that require further investigations, to be possible by combining experimental measurements with quantum chemical calculations.

Another interesting aspect is the reliability of the surface models representing the ice mantles. Among the reviewed works, they consisted of either minimal $(H_2O)_n$ (n = 1-4) clusters, in which the mobility of the H_2O molecules was at its maximum, larger clusters (n > 18-20), and only in the most recent works they were represented by amorphous clusters of hundreds of H_2O molecules, while adoption of periodic slab models is very scarce. However, as mentioned in the Computational Framework section, theoretical results can dramatically depend on the ice model and the evaluation of this aspect, *i.e.*, how results are actually affected by the structure and type of the ice model, should represent an important topic of future works dealing with iCOMs formation on atomistic ice models. Accordingly, comprehensive studies, and consistent from a methodological viewpoint, assessing the reliability of the different ice models and analyzing how similar/different are the results when using different ice models, are of great importance.

The role of water ice as catalyst has been clearly evidenced here. However, ice mantles are not limited to this role only. For instance, they can also act as reactant suppliers. In the reviewed works this role was shown when the reactants were also usual ice components, *e.g.*, H_2O itself or CO and NH_3. However, there are two other roles which have hardly been investigated. One is as reactant concentrator. Indeed, ice surfaces can immobilize and concentrate species, keeping them in close proximity for subsequent reactions. Assessing this role can be carried out by calculating the interaction energies between the reactants and the ice surfaces, which can indicate how strongly reactants are retained on the surfaces. Interaction energies were usually provided in most of the reviewed works but their relationship with the capability of surface ices to act as reactant suppliers is not usual. Another way to assess this role is by simulating the diffusivity of the reactive species.

This can be performed with AIMDs, in which retention times can be provided. Nevertheless, AIMD-based studies devoted to the diffusion properties of the reactants are very scarce. The other role is as third body, *i.e.*, ices quickly absorb the reaction energy excess, thereby stabilizing the product. This role can be investigated theoretically with AIMDs at NVE, in which the total energy E is conserved along the whole simulation. These simulations allow elucidating how the nascent reaction energies are partitioned, *i.e.*, what amount transforms into translational and internal energies of the product and what dissipates among the ice. Studies focused on this aspect are also very rare. Remarkably, the lack of this kind of works also evidences that use of AIMDs is very scarce in iCOMs formation investigations, a critical aspect since dynamic effects can be of great relevance especially in those reactions in which thermal heating is essential.

Finally, we address some words claiming for the need to simulate non-investigated reactions. Several important synthetic routes have indeed been simulated successfully but others, which are also important, are still missing. For instance, radical-radical couplings have scarcely been investigated: the $HCO\cdot + NH_2\cdot$ and $HCO\cdot + CH_3\cdot$ reactions have been simulated,[114,117] while other radical couplings are still to be studied. This is quite surprising since these reactions are assumed to be the main channels to form iCOMs usually detected in diverse astrophysical objects, as mentioned in the Introduction. In the same line, computational simulations have also been useful to identify new formation paths which are not normally accounted for in astrochemical modelling schemes (*e.g.*, $CN\cdot + H_2O$,[114]). Moreover, for some identified iCOMs, no reaction mechanisms have been proposed and simulated (*e.g.*, acetone $(CH_3)_2CO$ or vinyl alcohol $CH_2{=}CHOH$). Because of that, extensive quantum mechanical simulations devoted to novel “on-surface” formation paths to check their plausibility will be of great value. In relation to cometary and meteoritic biomolecules, the focus has been done essentially on glycine formation (while no simulations have been done for the rest of amino acids), on particular paths for nucleobases (but the NH_2CHO-based routes are unexplored yet), whereas sugars formation routes have not been addressed. Moreover,

understanding the role of the cometary and meteoritic minerals and ices will help us to get a better understanding on the origin of these compounds.

5 Acknowledgements

Albert Rimola is indebted to "Ramón y Cajal" program. This research was funded by MINECO (project CTQ2017-89132P), AGAUR (project 2017SGR1320), MIUR (Ministero dell'Istruzione, dell'Università e della Ricerca) and Scuola Normale Superiore (project PRIN 2015, STARS in the CAOS - Simulation Tools for Astrochemical Reactivity and Spectroscopy in the Cyberinfrastructure for Astrochemical Organic Species, cod. 2015F59J3R). This project has received funding from the European Research Council (ERC) under the European Union's Horizon 2020 research and innovation programme, for the Project "The Dawn of Organic Chemistry" (DOC), grant agreement No 741002.

6 Author's information

Corresponding author

Albert Rimola. Email: albert.rimola@uab.cat

Other authors

Lorenzo Zamirri. Email: lorenzo.zamirri@unito.it

Piero Ugliengo. Email: piero.ugliengo@unito.it

Cecilia Ceccarelli. Email: cecilia.ceccarelli@univ-grenoble-alpes.fr

ORCID

Lorenzo Zamirri: 0000-0003-0219-6150

Piero Ugliengo: 0000-0001-8886-9832

Albert Rimola: 0000-0002-9637-4554

Cecilia Ceccarelli: 0000-0001-9664-6292

7 References

(1) McGuire, B. A. 2018 Census of Interstellar, Circumstellar, Extragalactic, Protoplanetary Disk, and Exoplanetary Molecules. *Astrophys. J. Suppl. Ser.* **2018**, *239*, 17 (48 pp).

(2) Herbst, E.; van Dishoeck, E. F. Complex Organic Interstellar Molecules. *Annu. Rev. Astron. Astrophys.* **2009**, *47*, 427–480.

(3) Ceccarelli, C.; Caselli, P.; Fontani, F.; Neri, R.; López-Sepulcre, A.; Codella, C.; Feng, S.; Jiménez-Serra, I.; Lefloch, B.; Pineda, J. E.; et al. Seeds Of Life In Space (SOLIS): The Organic Composition Diversity at 300–1000 Au Scale in Solar-Type Star-Forming Regions. *Astrophys. J.* **2017**, *850*, 176 (15 pp).

(4) Ceccarelli, C.; Loinard, L.; Castets, A.; Faure, A.; Lefloch, B. Search for Glycine in the Solar Type Protostar IRAS 16293-2422. *Astron. Astrophys.* **2000**, *362*, 1122–1126.

(5) Cazaux, S.; Tielens, A. G. G. M.; Ceccarelli, C.; Castets, A.; Wakelam, V.; Caux, E.; Parise, B.; Teyssier, D. The Hot Core around the Low-Mass Protostar IRAS 16293-2422: Scoundrels Rule! *Astrophys. J.* **2003**, *593*, L51–L55.

(6) Ligterink, N. F. W.; Calcutt, H.; Coutens, A.; Kristensen, L. E.; Bourke, T. L.; Drozdovskaya, M. N.; Müller, H. S. P.; Wampfler, S. F.; van der Wiel, M. H. D.; van Dishoeck, E. F.; et al. The ALMA-PILS Survey: Stringent Limits on Small Amines and Nitrogen-Oxides towards IRAS 16293–2422B. *Astron. Astrophys.* **2018**, *619*, A28 (11 pp).

(7) Rubin, R. H.; Swenson, G. W., J.; Benson, R. C.; Tigelaar, H. L.; Flygare, W. H. Microwave Detection of Interstellar Formamide. *Astrophys. J.* **1971**, *169*, L39–L44.

(8) Charnley, S. B.; Tielens, A. G. G. M.; Millar, T. J. On the Molecular Complexity of the Hot Cores in Orion A-Grain Surface Chemistry as "The Last Refuge of the Scoundrel." *Astrophys. J.* **1992**, *339*, L71–L74.

(9) Balucani, N.; Ceccarelli, C.; Taquet, V. Formation of Complex Organic Molecules in Cold

Objects: The Role of Gas-Phase Reactions. *Mon. Not. R. Astron. Soc.* **2015**, *449*, L16–L20.

(10) Charnley, S. B.; Herbst, E. Reactive Desorption and Radiative Association as Possible Drivers of Complex Molecule Formation in the Cold Interstellar Medium. *Astrophys. J.* **2013**, *769*, 34 (9 pp).

(11) Garrod, R. T.; Herbst, E. Formation of Methyl Formate and Other Organic Species in the Warm-up Phase of Hot Molecular Cores. *Astron. Astrophys.* **2006**, *457*, 927–936.

(12) Öberg, K. I.; Garrod, R. T.; Dishoeck, E. F. van; Linnartz, H. Formation Rates of Complex Organics in UV Irradiated CH3OH-Rich Ices. I. Experiments. *Astron. Astrophys.* **2009**, *504*, 891–913.

(13) Ruaud, M.; Loison, J. C.; Hickson, K. M.; Gratier, P.; Hersant, F.; Wakelam, V. Modelling Complex Organic Molecules in Dense Regions: Eley–Rideal and Complex Induced Reaction. *Mon. Not. R. Astron. Soc.* **2015**, *447*, 4004–4017.

(14) Watanabe, N.; Kouchi, A. Efficient Formation of Formaldehyde and Methanol by the Addition of Hydrogen Atoms to CO in H_2O-CO Ice at 10 K. *Astrophys. J. Lett.* **2002**, *571*, L173–L176.

(15) Rimola, A.; Taquet, V.; Ugliengo, P.; Balucani, N.; Ceccarelli, C. Astrophysics Combined Quantum Chemical and Modeling Study of CO Hydrogenation on Water Ice. *Astron. Astrophys.* **2014**, *572*, A70.

(16) Jones, A. P.; Fanciullo, L.; Kohler, M.; Verstraete, L.; Guillet, V.; Bocchio, M.; Ysard, N. The Evolution of Amorphous Hydrocarbons in the ISM: Dust Modelling from a New Vantage Point. *Astron. Astrophys.* **2014**, *558*, 22.

(17) Henning, T. Cosmic Silicates. *Annu. Rev. Astron. Astrophys.* **2010**, *48*, 21–46.

(18) Jones, A. P.; Köhler, M.; Ysard, N.; Bocchio, M.; Verstraete, L. The Global Dust Modelling Framework THEMIS. *Astron. Astrophys.* **2017**, *602*, A46 (9 pp).

(19) Whittet, D. C. B.; Schutte, W. A.; Tielens, A. G. G. M.; Boogert, A. C. A.; de Graauw, T.; Ehrenfreund, P.; Gerakines, P. A.; Helmich, F. P.; Prusti, T.; van Dishoeck, E. F. An ISO SWS View of Interstellar Ices: First Results. *Astron. Astrophys.* **1996**, *360*, L357–L360.

(20) Boogert, A. C. A.; Gerakines, P. A.; Whittet, D. C. B. Observations of the Icy Universe. *Annu. Rev. Astron. Astrophys.* **2015**, *53*, 541–583.

(21) Watanabe, N.; Kouchi, A. Ice Surface Reactions: A Key to Chemical Evolution in Space. *Prog. Surf. Sci.* **2008**, *83*, 439–489.

(22) Fraser, H. J.; Collings, M. P.; Dever, J. W.; McCoustra, M. R. S. Using Laboratory Studies of CO-H_2O Ices to Understand the Non-Detection of a 2152 cm^{-1} (4.647 μm) Band in the Spectra of Interstellar Ices. *Mon. Not. R. Astron. Soc.* **2004**, *353*, 59–68.

(23) Zamirri, L.; Casassa, S.; Rimola, A.; Segado-Centellas, M.; Ceccarelli, C.; Ugliengo, P. IR Spectral Fingerprint of Carbon Monoxide in Interstellar Water Ice Models. *Mon. Not. R. Astron. Soc.* **2018**, *480*, 1427–1444.

(24) McGuire, B. A.; Shingledecker, C. N.; Willis, E. R.; Burkhardt, A. M.; El-Abd, S.; Motiyenko, R. A.; Brogan, C. L.; Hunter, T. R.; Margulès, L.; Guillemin, J.-C.; et al. ALMA Detection of Interstellar Methoxymethanol (CH_3OCH_2OH). *Astrophys. J. Lett.* **2017**, *851*, L46 (8 pp).

(25) Linnartz, H.; Ioppolo, S.; Fedoseev, G. Atom Addition Reactions in Interstellar Ice Analogues. *Int. Rev. Phys. Chem.* **2015**, *34*, 205–237.

(26) Barone, V.; Latouche, C.; Skouteris, D.; Vazart, F.; Balucani, N.; Ceccarelli, C.; Lefloch, B. Gas-Phase Formation of the Prebiotic Molecule Formamide: Insights from New Quantum Computations. *Mon. Not. R. Astron. Soc.* **2015**, *453*, L31–L35.

(27) Vazart, F.; Calderini, D.; Puzzarini, C.; Skouteris, D.; Barone, V. State-of-the-Art Thermochemical and Kinetic Computations for Astrochemical Complex Organic Molecules:

Formamide Formation in Cold Interstellar Clouds as a Case Study. *J. Chem. Theory Comput.* **2016**, *12*, 5385–5397.

(28) Skouteris, D.; Vazart, F.; Ceccarelli, C.; Balucani, N.; Puzzarini, C.; Barone, V. New Quantum Chemical Computations of Formamide Deuteration Support Gas-Phase Formation of This Prebiotic Molecule. *Mon. Not. R. Astron. Soc.* **2017**, *468*, L1–L5.

(29) Wakelam, V.; Loison, J.; Mereau, R.; Ruaud, M. Binding Energies : New Values and Impact on the Efficiency of Chemical Desorption. *Mol. Astrophys.* **2017**, *6*, 22–35.

(30) Holtom, P. D.; Bennett, C. J.; Osamura, Y.; Mason, N. J.; Kaiser, R. I. A Combined Experimental and Theoretical Study on the Formation of the Amino Acid Glycine (NH_2CH_2COOH) and Its Isomer ($CH_3NHCOOH$) in Extraterrestrial Ices. *Astrophys. J.* **2005**, *626*, 940–952.

(31) Walch, S. P.; Bauschlicher Jr, C. B.; Ricca, A.; Bakes, E. L. O. On the Reaction CH_2O + $NH_3 \rightarrow CH_2NH$ + H2O. *Chem. Phys. Lett.* **2001**, *333*, 6–11.

(32) Redondo, P.; Barrientos, C.; Largo, A. Some Insights into Formamide Formation through Gas-Phase Reactions in the Interstellar Medium. *Astrophys. J.* **2013**, *780*, 181 (7 pp).

(33) Huang, L. C. L.; Asvany, O.; Chang, A. H. H.; Balucani, N.; Lin, S. H.; Lee, Y. T.; Kaiser, R. I. Crossed Beam Reaction of Cyano Radicals with Hydrocarbon Molecules. IV. Chemical Dynamics of Cyanoacetylene (HCCCN; X $^1\Sigma^+$) Formation from Reaction of CN(X $^2\Sigma^+$) with Acetylene, C_2H_2(X $^1\Sigma_g^+$). *J. Chem. Phys.* **2000**, *113*, 8656–8666.

(34) Navarro-Ruiz, J.; Sodupe, M.; Ugliengo, P.; Rimola, A. Interstellar H Adsorption and H_2 Formation on the Crystalline (010) Forsterite Surface: A B3LYP-D2* Periodic Study. *Phys. Chem. Chem. Phys.* **2014**, *16*, 17447–17457.

(35) Navarro-Ruiz, J.; Ugliengo, P.; Sodupe, M.; Rimola, A. Does Fe^{2+} in Olivine-Based Interstellar Grains Play Any Role in the Formation of H2? Atomistic Insights from DFT

Periodic Simulations. *Chem. Commun.* **2016**, *52*, 6873–6876.

(36) Navarro-Ruiz, J.; Martínez-González, J. Á.; Sodupe, M.; Ugliengo, P.; Rimola, A. Relevance of Silicate Surface Morphology in Interstellar H2 Formation. Insights from Quantum Chemical Calculations. *Mon. Not. R. Astron. Soc.* **2015**, *453*, 914–924.

(37) Molpeceres, G.; Rimola, A.; Ceccarelli, C.; Kästner, J.; Ugliengo, P.; Maté, B. Silicate-Mediated Interstellar Water Formation: A Theoretical Study. *Mon. Not. R. Astron. Soc.* **2019**, *482*, 5389–5400.

(38) Sherrill, C. D. Frontiers in Electronic Structure Theory. *J. Chem. Phys.* **2010**, *132*, 110902 (7 pp).

(39) Řezáč, J.; Hobza, P. Describing Noncovalent Interactions beyond the Common Approximations: How Accurate Is the "Gold Standard", CCSD(T) at the Complete Basis Set Limit? *J. Chem. Theory Comput.* **2013**, *9*, 2151–2155.

(40) Sousa, S. F.; Fernandes, P. A.; Ramos, M. J. General Performance of Density Functionals. *J. Phys. Chem. A* **2007**, *111*, 10439–10452.

(41) Cramer, C. J.; Truhlar, D. G. Density Functional Theory for Transition Metals and Transition Metal Chemistry. *Phys. Chem. Chem. Phys.* **2009**, *11*, 10757–10816.

(42) Hao, P.; Sun, J.; Xiao, B.; Ruzsinszky, A.; Csonka, G. I.; Tao, J.; Glindmeyer, S.; Perdew, J. P. Performance of Meta-GGA Functionals on General Main Group Thermochemistry, Kinetics, and Noncovalent Interactions. *J. Chem. Theory Comput.* **2013**, *9*, 355–363.

(43) Kroes, G.-J. Toward a Database of Chemically Accurate Barrier Heights for Reactions of Molecules with Metal Surfaces. *J. Phys. Chem. Lett.* **2016**, *6*, 4106–4114.

(44) Grimme, S. Density Functional Theory with London Dispersion Corrections. *WIREs Comput. Mol. Sci.* **2011**, *1*, 211–228.

(45) Cramer, C. J. *Essentials of Computational Chemistry*; 2004.

(46) Jensen, F. *Introduction to Computational Chemistry*; 2007.

(47) Atkins, P.; de Paula, J. *Chemical Physics*; 2010.

(48) Shimonishi, T. Adsorption Energies of Carbon, Nitrogen, and Oxygen Atoms on the Low-Temperature Amorphous Water Ice: A Systematic Estimation from Quantum Chemistry Calculations. *Astrophys. J.* **2018**, *855*, 27 (11 pp).

(49) Song, L.; Kästner, J. Formation of the Prebiotic Molecule NH_2CHO on Astronomical Amorphous Solid Water Surfaces: Accurate Tunneling Rate Calculations. *Phys. Chem. Chem. Phys.* **2016**, *18*, 29278–29285.

(50) Al-Halabi, A.; Fraser, H. J.; Kroes, G. J.; van Dishoeck, E. F. Adsorption of CO on Amorphous Water-Ice Surfaces. *Astron. Astrophys.* **2004**, *422*, 777–791.

(51) Goldman, N.; Reed, E. J.; Fried, L. E.; Kuo, I. W.; Maiti, A. Synthesis of Glycine-Containing Complexes in Impacts of Comets on Early Earth. *Nat. Chem.* **2010**, *2*, 949–954.

(52) Goldman, N.; Tamblyn, I. Prebiotic Chemistry within a Simple Impacting Icy Mixture. *J. Phys. Chem. A* **2013**, *117*, 5124–5131.

(53) Laidler, K. J.; King, M. C. Development of Transition-State Theory. *J. Phys. Chem.* **1983**, *87*, 2657–2664.

(54) Eyring, H. The Activated Complex in Chemical Reactions. *J. Chem. Phys.* **1935**, *3*, 107–115.

(55) Evans, M. G.; Polanyi, M. Some Applications of the Transition State Method to the Calculation of Reaction Velocities, Especially in Solution. *Trans. Faraday Soc.* **1935**, *31*, 875–894.

(56) Williams, D. A. The Interstellar Medium: An Overview. In *Solid State Astrochemistry*; Pirronello, V., Krelowski, J., Manicò, G., Eds.; Proceedings of the NATO Advanced Study

Institute on Solid State Astrochemistry, 2000; pp 1–20.

(57) Larson, R. B. The Evolution of Molecular Clouds. **1993**.

(58) Meisner, J.; Kästner, J. Atom Tunneling in Chemistry. *Angew. Chemie Int. Ed.* **2016**, *55*, 5400–5413.

(59) Eckart, C. The Penetration of a Potential Barrier by Electrons. *Phys. Rev.* **1930**, *35*, 1303–1309.

(60) Miller, W. H. Semiclassical Limit of Quantum Mechanical Transition State Theory for Nonseparable Systems. *J. Chem. Phys.* **1975**, *62*, 1899–1906.

(61) Richardson, J. O. Derivation of Instanton Rate Theory from First Principles. *J. Chem. Phys.* **2016**, *144*, 114106 (5 pp).

(62) Andersson, S.; Nyman, G.; Arnaldsson, A.; Manthe, U.; Jónsson, H. Comparison of Quantum Dynamics and Quantum Transition State Theory Estimates of the H + CH4 Reaction Rate. *J. Phys. Chem. A* **2009**, *113*, 4468–4478.

(63) Feynman, R. P. Space-Time Approach to Non-Relativistic Quantum Mechanics. *Rev. Mod. Phys.* **1948**, *20*, 367–387.

(64) Song, L.; Kästner, J. Formation of the Prebiotic Molecule NH2CHO on Astronomical Amorphous Solid Water Surfaces: Accurate Tunneling Rate Calculations. *Phys. Chem. Chem. Phys.* **2016**, *18*, 29278–29285.

(65) Rommel, J. B.; Goumans, T. P. M.; Kästner, J. Locating Instantons in Many Degrees of Freedom. *J. Chem. Theory Comput.* **2011**, *7*, 690–698.

(66) McQuarrie, D. A.; Simon, J. D. *Physical Chemistry. A Molecular Approach*; University Science Books: Sausalito, CA, USA, 1997.

(67) Demichelis, R.; Bruno, M.; Massaro, F. R.; Prencipe, M.; de la Pierre, M.; Nestola, F. First-

Principle Modelling of Forsterite Surface Properties: Accuracy of Methods and Basis Sets. *J. Comput. Chem.* **2015**, *36*, 1439–1445.

(68) Mukhopadhyay, S.; Bailey, C. L.; Wander, A.; Searle, B. G.; Muryn, C. A. Stability of the AlF_3 (0 0 -1 2) Surface in H_2O and HF Environments: An Investigation Using Hybrid Density Functional Theory and Atomistic Thermodynamics. *Surf. Sci.* **2007**, *601*, 4433–4437.

(69) Bailey, C. L.; Mukhopadhyay, S.; Wander, A.; Searle, B. G.; Harrison, N. M. Structure and Stability of α-AlF3 Surfaces. *J. Phys. Chem. C* **2009**, *113*, 4976–4983.

(70) Zamirri, L.; Corno, M.; Rimola, A.; Ugliengo, P. Forsterite Surfaces as Models of Interstellar Core Dust Grains: Computational Study of Carbon Monoxide Adsorption. *ACS Earth Sp. Chem.* **2017**, *1*, 384–398.

(71) Chiatti, F.; Corno, M.; Sakhno, Y.; Martra, G.; Ugliengo, P. Revealing Hydroxyapatite Nanoparticle Surface Structure by CO Adsorption: A Combined B3LYP and Infrared Study. *J. Phys. Chem. C* **2013**, *117*, 25526–25534.

(72) Boese, A. D.; Sauer, J. Accurate Adsorption Energies for Small Molecules on Oxide Surfaces: CH_4/MgO(001) and C_2H_6/MgO(001). *J. Comput. Chem.* **2016**, *37*, 2374–2385.

(73) Boese, A. D.; Sauer, J. Accurate Adsorption Energies of Small Molecules on Oxide Surfaces: CO-MgO(001). *Phys. Chem. Chem. Phys.* **2013**, *15*, 16481–16493.

(74) Escamilla-Roa, E.; Moreno, F. Adsorption of Glycine on Cometary Dust Grains: II — Effect of Amorphous Water Ice. *Planet. Space Sci.* **2013**, *75*, 1–10.

(75) Escamilla-Roa, E.; Moreno, F. Adsorption of Glycine by Cometary Dust: Astrobiological Implications. *Planet. Space Sci.* **2012**, *70*, 1–9.

(76) Al-Halabi, A.; Kleyn, A. W.; Van Dishoeck, E. F.; Van Hemert, M. C.; Kroes, G. J. Sticking of Hyperthermal CO to the (0001) Face of Crystalline Ice. *J. Phys. Chem. A* **2003**, *107*,

10615–10624.

(77) Civalleri, B.; Maschio, L.; Ugliengo, P.; Zicovich-Wilson, C. M. Role of Dispersive Interactions in the CO Adsorption on MgO(001): Periodic B3LYP Calculations Augmented with an Empirical Dispersion Term. *Phys. Chem. Chem. Phys.* **2010**, *12*, 6382–6389.

(78) Pisani, C.; Schütz, M.; Casassa, S.; Usvyat, D.; Maschio, L.; Lorenz, M.; Erba, A. CRYSCOR: A Program for the Post-Hartree–Fock Treatment of Periodic Systems. *Phys. Chem. Chem. Phys.* **2012**, *14*, 7615–7628.

(79) Chung, L. W.; Sameera, W. M. C.; Ramozzi, R.; Page, A. J.; Hatanaka, M.; Petrova, G. P.; Harris, T. V.; Li, X.; Ke, Z.; Liu, F.; et al. The ONIOM Method and Its Applications. *Chem. Rev.* **2015**, *115*, 5678–5796.

(80) Svensson, M.; Humbel, S.; Froese, R. D. J.; Matsubara, T.; Sieber, S.; Morokuma, K. ONIOM: A Multi-Layered Integrated MO + MM Method for Geometry Optimizations and Single Point Energy Predictions. A Test for Diels-Alder Reactions and $Pt(P(t\text{-}Bu)_3)_2+H_2O$ Oxidative Addition. *J. Phys. Chem.* **1996**, *100*, 19357–19363.

(81) Dapprich, S.; Komáromi, I.; Byun, K. S.; Morokuma, K.; Frisch, M. J. A New ONIOM Implementation in Gaussian 98. 1. The Calculation of Energies, Gradients and Vibrational Frequencies and Electric Field Derivatives. *J. Mol. Struct.* **1999**, *462*, 1–21.

(82) Collings, M. P.; Frankland, V. L.; Lasne, J.; Marchione, D.; Rosu-Finsen, A.; McCoustra, M. R. S. Probing Model Interstellar Grain Surfaces with Small Molecules. *Mon. Not. R. Astron. Soc.* **2015**, *449*, 1826–1833.

(83) Collings, M. P.; Anderson, M. A.; Chen, R.; Dever, J. W.; Viti, S.; Williams, D. A.; McCoustra, M. R. S. A Laboratory Survey of the Thermal Desorption of Astrophysically Relevant Molecules. *Mon. Not. R. Astron. Soc.* **2004**, *354*, 1133–1140.

(84) Garrod, R. T. Three-Dimensional, Off-Lattice Monte Carlo Kinetcs Simulations of

Interstellar Grain Chemistry and Ice Structure. *Astron. J.* **2013**, *778*, 150 (14 pp).

(85) Sandford, S. A.; Allamandola, L. J.; Tielens, A. G. G. M.; Valero, G. J. Laboratory Studies of the Infrared Spectral Properties of CO in Astrophysical Ices. *Astrophys. J.* **1988**, *329*, 498–510.

(86) Dendy Sloan Jr., E.; Koh, C. A. *Clathrate Hydrates of Natural Gases*; CRC Press: Boca Raton, FL, USA, 2007.

(87) Loveday, J. S.; Nelmes, R. J.; Guthrie, M.; Belmonte, S. A.; Allan, D. R.; Klug, D. D.; Tse, J. S.; Handa, Y. P. Stable Methane Hydrate above 2 GPa and the Source of Titan's Atmospheric Methane. *Nature* **2001**, *410*, 661–663.

(88) Davidson, D. W.; Desando, M. A.; Cough, S. R.; Handa, Y. P.; Ratcliff, C. I.; Ripmeester, J. A.; Tse, J. S. A Clathrate Hydrate of Carbon Monoxide. *Nature* **1987**, *328*, 418–419.

(89) Cossi, M.; Rega, N.; Scalmani, G.; Barone, V. Energies, Structures, and Electronic Properties of Molecules in Solution with the C-PCM Solvation Model. *J. Comput. Chem.* **2003**, *24*, 669–681.

(90) Tomasi, J.; Mennucci, B.; Cammi, R. Quantum Mechanical Continuum Solvation Models. *Chem. Rev.* **2005**, *105*, 2999–3094.

(91) Woon, D. E. Ab Initio Quantum Chemical Studies of Reactions in Astrophysical Ices. 4. Reactions in Ices Involving HCOOH, CH_2NH, HCN, HNC, NH_3 , and H_2O. *Int. J. Quantum Chem.* **2002**, *88*, 226–235.

(92) Koch, D. M.; Toubin, C.; Peslherbe, G. H.; Hynes, J. T. A Theoretical Study of the Formation of the Aminoacetonitrile Precursor of Glycine on Icy Grain Mantles in the Interstellar Medium. *J. Phys. Chem. C* **2008**, *112*, 2972–2980.

(93) Riffet, V.; Frison, G.; Bouchoux, G. Quantum-Chemical Modeling of the First Steps of the Strecker Synthesis: From the Gas-Phase to Water Solvation. *J. Phys. Chem. A* **2018**, *122*,

1643–1657.

(94) Koch, D. M.; Toubin, C.; Xu, S.; Peslherbe, G. H.; Hynes, J. T. Concerted Proton-Transfer Mechanism and Solvation Effects in the HNC/HCN Isomerization on the Surface of Icy Grain Mantles in the Interstellar Medium. *J. Phys. Chem. C* **2007**, *111*, 15026–15033.

(95) Tielens, A. G. G. M.; Hagen, W. Model Calculations of the Molecular Composition of Interstellar Grain Mantles. *Astron. Astrophys.* **1982**, *114*, 245–260.

(96) Pirim, C.; Krim, L.; Laffon, C.; Parent, P.; Pauzat, F.; Pilmé, J.; Ellinger, Y. Preliminary Study of the Influence of Environment Conditions on the Successive Hydrogenations of CO. *J. Phys. Chem. A* **2010**, *114*, 3320–3328.

(97) Woon, D. E. Modeling Gas-Grain Chemistry with Quantum Chemical Cluster Calculations. I. Heterogeneous Hydrogenation of CO and H2CO on Icy Grain Mantles. *Astrophys. J.* **2002**, *569*, 541–548.

(98) Rimola, A.; Taquet, V.; Ugliengo, P.; Balucani, N.; Ceccarelli, C. Combined Quantum Chemical and Modeling Study of CO Hydrogenation on Water Ice. *Astron. Astrophys.* **2014**, *572*, A70 (12 pp).

(99) Goumans, T. P. M.; Wander, A.; Catlow, C. R. A.; Brown, W. A. Silica Grain Catalysis of Methanol Formation. *Mon. Not. R. Astron. Soc.* **2007**, *1832*, 1829–1832.

(100) Goumans, T. P. M.; Catlow, C. R. A.; Brown, W. A. Hydrogenation of CO on a Silica Surface: An Embedded Cluster Approach. *J. Chem. Phys.* **2008**, *128*, 134709.

(101) Woon, D. E. Ion-Ice Astrochemistry: Barrierless Low-Energy Deposition Pathways to HCOOH, CH3OH, and CO_2 on Icy Grain Mantles from Precursor Cations. *Astrophys. J.* **2011**, *728*, 44–49.

(102) Töpfer, M.; Jusko, P.; Schlemmer, S.; Asvany, O. Double Resonance Rotational Spectroscopy of CH_2D^+. *Astron. Astrophys.* **2016**, *593*, L11–L14.

(103) Roueff, E.; Gerin, M.; Lis, D. C.; Wootten, A.; Marcelino, N.; Cernicharo, J.; Tercero, B. CH_2D^+, the Search for the Holy Grail. *J. Phys. Chem. A* **2013**, *117*, 9959–9967.

(104) Bisschop, S. E.; Jørgensen, J. K.; van Dishoeck, E. F.; de Wachter, E. B. M. Testing Grain-Surface Chemistry in Massive Hot-Core Regions. *Astron. Astrophys.* **2007**, *465*, 913–929.

(105) Kahane, C.; Ceccarelli, C.; Faure, A.; Caux, E. Detection of Formamide, the Simplest but Crucial Amide, in a Solar-Type Protostar. *Astrophys. J. Lett.* **2013**, *763*, L38 (5 pp).

(106) López-Sepulcre, A.; Jaber, A. A.; Mendoza, E.; Lefloch, B.; Ceccarelli, C.; Vastel, C.; Bachiller, R.; Cernicharo, J.; Codella, C.; Kahane, C.; et al. Shedding Light on the Formation of the Pre-Biotic Molecule Formamide with ASAI. *Mon. Not. R. Astron. Soc.* **2015**, *449*, 2438–2458.

(107) Takahiro, Y.; Takano, S.; Watanabe, Y.; Sakai, N.; Sakai, T.; Liu, S.-Y.; Su, Y.-N.; Hirano, N.; Takakuwa, S.; Aikawa, Y.; et al. The 3 mm Spectral Line Survey toward the Lynds 1157 B1 Shocked Region. I. Data. *Publ. Astron. Soc. Japan* **2012**, *64*, 105 (45 pp).

(108) Codella, C.; Ceccarell, C.; Caselli, P.; Balucani, N.; Barone, V.; Fontani, F.; Lefloch, B.; Podio, L.; Viti, S.; Feng, S.; et al. Seeds of Life in Space (SOLIS) II. Formamide in Protostellar Shocks: Evidence for Gas-Phase Formation. *Astron. Astrophys.* **2017**, *605*, L3 (7 pp).

(109) Bianchi, E.; Codella, C.; Ceccarelli, C.; Vazart, F.; Bachiller, R.; Balucani, N.; Bouvier, M.; Simone, M. De; Enrique-Romero, J.; Kahane, C.; et al. The Census of Interstellar Complex Organic Molecules in the Class I Hot Corino of SVS13-A. *Mon. Not. R. Astron. Soc.* **2019**, *483*, 1850–1861.

(110) Bockelée-Morvan, D.; Lis, D. C.; Wink, J. E.; Despois, D.; Crovisier, J.; Bachiller, R.; Benford, D. J.; Biver, N.; Colom, P.; Davies, J. K.; et al. New Molecules Found in Comet C/1995 O1 (Hale-Bopp) Investigating the Link between Cometary and Interstellar Material.

Astron. Astrophys. **2000**, *353*, 1101–1114.

(111) Biver, N.; Bockelée-Morvan, D.; Moreno, R.; Crovisier, J.; Colom, P.; Lis, D. C.; Sandqvist, A.; Boissier, J.; Despois, D.; Milam, S. N. Ethyl Alcohol and Sugar in Comet C/2014 Q2 (Lovejoy). *Sci. Adv.* **2015**, *1*, 1–5.

(112) Spezia, R.; Jeanvoine, Y.; Hase, W. L.; Song, K.; Largo, A. Synthesis of Formamide and Related Organic Species in the Interstellar Medium via Chemical Dynamics Simulations. *Astrophys. J.* **2016**, *826*, 107 (8 pp).

(113) Noble, J. A.; Theule, P.; Congiu, E.; Dulieu, F.; Bonnin, M.; Bassas, A.; Duvernay, F.; Danger, G.; Chiavassa, T. Hydrogenation at Low Temperatures Does Not Always Lead to Saturation: The Case of HNCO. *Astron. Astrophys.* **2015**, *9*, A91 (9 pp).

(114) Rimola, A.; Skouteris, D.; Balucani, N.; Ceccarelli, C.; Enrique-Romero, J.; Taquet, V.; Ugliengo, P. Can Formamide Be Formed on Interstellar Ice? An Atomistic Perspective. *ACS Earth Sp. Chem.* **2018**, *2*, 720–734.

(115) Garrod, R. T.; Weaver, S. L. W.; Herbst, E. Complex Chemistry in Star-Forming Regions: An Expanded Gas-Grain Warm-up Chemical Model. *Astrophys. J.* **2008**, *682*, 283–302.

(116) Öberg, K. I. Photochemistry and Astrochemistry: Photochemical Pathways to Interstellar Complex Organic Molecules. *Chem. Rev.* **2016**, *116*, 9631–9663.

(117) Enrique-Romero, J.; Rimola, A.; Ceccarelli, C.; Balucani, N. The (Impossible ?) Formation of Acetaldehyde on the Grain Surfaces: Insights from Quantum Chemical Calculations. *Mon. Not. R. Astron. Soc.* **2016**, *459*, L6–L10.

(118) Bredehoft, J. H.; Bohler, E.; Schmidt, F.; Borrmann, T.; Swiderek, P. Electron-Induced Synthesis of Formamide in Condensed Mixtures of Carbon Monoxide and Ammonia. *ACS Earth Sp. Chem.* **2017**, *1*, 59–59.

(119) Woon, D. E. Pathways to Glycine and Other Amino Acids in Ultraviolet-Irradiated

Astrophysical Ices Determined via Quantum Chemical Modeling. *Astrophys. J.* **2002**, *571*, L177–L180.

(120) Rimola, A.; Sodupe, M.; Ugliengo, P. Computational Study of Interstellar Glycine Formation Occurring at Radical Surfaces of Water-Ice Dust Particles. *Astron. J.* **2012**, *754*, 24–33.

(121) Park, J.; Woon, D. E. Theoretical Modeling of Formic Acid (HCOOH), FORMATE ($HCOO^-$), and Ammonium (NH_4^+) Vibrational Spectra in Astrophysical Ices. *Astrophys. J.* **2006**, *648*, 1285–1290.

(122) Kayi, H.; Kaiser, R. I.; Head, J. D. A Computational Study on the Structures of Methylamine–carbon Dioxide–water Clusters: Evidence for the Barrier Free Formation. *Phys. Chem. Chem. Phys.* **2011**, *13*, 11083–11098.

(123) Park, J.; Woon, D. E. Theoretical Investigation of OCN– Charge-Transfer Complexes in Condensed-Phase Media: Spectroscopic Properties in Amorphous Ice. *J. Phys. Chem. A* **2004**, *108*, 6589–6598.

(124) Park, J.; Woon, D. E. Computational Confirmation of the Carrier for the "XCN" Interstellar Ice Band: OCN– Charge Transfer Complexes. *Astron. J.* **2004**, *601*, L63–L66.

(125) Snyder, L. E. .; Buhl, D. Observations of Radio Emission from Interstellar Hydrogen Cyanide. *Astrophys. J.* **1971**, *163*, L47–L52.

(126) Schilke, P. .; Comito, C. .; Thorwirth, S. First Detection of Vibrationally Excited HNC in Space. *Astrophys. J.* **2003**, *582*, L101–L104.

(127) Gardebien, F.; Sevin, A. Catalytic Model Reactions for the HCN Isomerization. I. Theoretical Characterization of Some Water-Catalyzed Mechanisms. *J. Phys. Chem. A* **2003**, *107*, 3925–3934.

(128) Woon, D. E. A Quantum Chemical Study of the Formation of Cyanide (CN^-) and Acetate ($CH3COO^-$) Ions in Astrophysical Ices via Proton Transfer from HCN, HNC, or CH_3COOH

to NH_3. *Comput. Theor. Chem.* **2012**, *984*, 108–112.

(129) Woon, D. E. Ab Initio Quantum Chemical Studies of Reactions in Astrophysical Ices. 1. Amminolysis, Hydrolysis and Polymerization in $H_2CO/NH_3/H_2O$ Ices. *Icarus* **1999**, *142*, 550–556.

(130) Woon, D. E. Ab Initio Quantum Chemical Studies of Reactions in Astrophysical Ices 3. Reactions of HOCH2NH2 Formed in $H_2CO/NH_3/H_2O$ Ices. *J. Phys. Chem. A* **2001**, *105*, 9478–9481.

(131) Courmier, D.; Gardebien, F.; Minot, C.; St-Amant, A. A Computational Study of the Water-Catalyzed Formation of NH2CH2OH. *Chem. Phys. Lett.* **2005**, *405*, 357–363.

(132) Rimola, A.; Sodupe, M.; Ugliengo, P. Deep-Space Glycine Formation via Strecker-Type Reactions Activated by Ice Water Dust Mantles. A Computational Approach. *Phys. Chem. Chem. Phys.* **2010**, *12*, 5285–5294.

(133) Chen, L.; Woon, D. E. A Theoretical Investigation of the Plausibility of Reactions between Ammonia and Carbonyl Species (Formaldehyde, Acetaldehyde, and Acetone) in Interstellar Ice Analogs at Ultracold Temperatures. *J. Phys. Chem. A* **2011**, *115*, 5166–5183.

(134) Duvernay, F.; Rimola, A.; Theule, P.; Danger, G.; Sanchez, T.; Chiavassa, T. Formaldehyde Chemistry in Cometary Ices: The Case of $HOCH_2OH$ Formation. *Phys. Chem. Chem. Phys.* **2014**, *16*, 24200–24208.

(135) Fresneau, A.; Danger, G.; Rimola, A.; Duvernay, F.; Theulé, P.; Chiavassa, T. Ice Chemistry of Acetaldehyde Reveals Competitive Reactions in the First Step of the Strecker Synthesis of Alanine Formation of $HO–CH(CH_3)–NH_2$. *Mon. Not. R. Astron. Soc.* **2015**, *451*, 1649–1660.

(136) Fresneau, A.; Danger, G.; Rimola, A.; Theulé, P.; Duvernay, F.; Chiavassa, T. Trapping in Water - an Important Prerequisite for Complex Reactivity in Astrophysical Ices: The Case of Acetone $(CH_3)_2C=O$ and Ammonia NH_3. *Mon. Not. R. Astron. Soc.* **2014**, *443*, 2991–3000.

(137) Snyder, L. E.; Buhl, D.; Zuckerman, B.; Palmer, P. Microwave Detection of Interstellar Formaldehyde. *Phys. Rev. Lett.* **1969**, *22*, 679–681.

(138) Zeng, S.; Quénard, D.; Jiménez-Serra, I.; Martín-Doménech, J Martín-Pintado, V. M.; L, R.; R, T. First Detection of the Pre-Biotic Molecule Glycolonitrile ($HOCH_2CN$) in the Interstellar Medium. *Mon. Not. R. Astron. Soc.* **2019**, *484*, L43–L48.

(139) Woon, D. E. Ab Initio Quantum Chemical Studies of Reactions in Astrophysical Ices. *Icarus* **2001**, *149*, 277–284.

(140) Danger, G.; Rimola, A.; Mrad, N. A.; Duvernay, F.; Roussin, G.; Theule, P.; Chiavassa, T. Formation of Hydroxyacetonitrile ($HOCH_2CN$) and Polyoxymethylene (POM)-Derivatives in Comets from Formaldehyde (CH_2O) and Hydrogen Cyanide (HCN) Activated by Water. *Phys. Chem. Chem. Phys.* **2014**, *16*, 3360–3370.

(141) Fresneau, A.; Danger, G.; Rimola, A.; Duvernay, F.; Theulé, P.; Chiavassa, T. Thermal Formation of Hydroxynitriles, Precursors of Hydroxyacids in Astrophysical Ice Analogs: Acetone ($(CH_3)_2CO$) and Hydrogen Cyanide (HCN) Reativity. *Mol. Astrophys.* **2015**, *1*, 1–12.

(142) Belloche, A.; Menten, K. M.; Comito, C.; Müller, H. S. P.; Schilke, P.; Ott, J.; Thorwirth, S.; Hieret, C. Detection of Amino Acetonitrile in SgRB2(N). *Astron. Astrophys.* **2008**, *492*, 769–773.

(143) Elsila, J. E.; Glavin, D. P.; Dworkin, J. P. Cometary Glycine Detected in Samples Returned by Stardust. *Meteorit. Planet. Sci.* **2010**, *44*, 1323–1330.

(144) Sandford, S. A.; Aléon, J.; Alexander, C. M.; Araki, T.; Bajt, S.; Baratta, G. A.; Borg, J.; Bradley, J. P.; Brownlee, D. E.; Brucato, J. R.; et al. Organics Captured from Comet 81P/Wild 2 by the Stardust Spacecraft. *Science* **2006**, *314*, 1720–1724.

(145) Altwegg, K.; Balsiger, H.; Bar-Nun, A.; Berthelier, J.-J.; Bieler, A.; Bochsler, P.; Briois, C.;

Calmonte, U.; Combi, M. R.; Cottin, H.; et al. Prebiotic Chemicals – Amino Acid and Phosphorus – in the Coma of Comet 67P/Churyumov-Gerasimenko. *Sci. Adv.* **2016**, *2*, 5 pp.

(146) Pizzarello, S. The Chemistry of Life's Origin: A Carbonaceous Meteorite Perspective. *Acc. Chem. Res.* **2006**, *39*, 231–237.

(147) Strecker, A. Ueber Die Künstliche Bildung Der Milchsäure Und Einen Neuen, Dem Glycocoll Homologen Körper. *Ann. der Chemie und Pharm.* **1850**, *75*, 27–45.

(148) Nhlabatsi, Z. P.; Bhasi, P.; Sitha, S. Possible Interstellar Formation of Glycine from the Reaction of CH2=NH, CO and H2O: Catalysis by Extra Water Molecules through the Hydrogen Relay Transport. *Phys. Chem. Chem. Phys.* **2016**, *18*, 375–381.

(149) Nhlabatsi, Z. P.; Bhasi, P.; Sitha, S. Possible Interstellar Formation of Glycine through a Concerted Mechanism: A Computational Study on the Reaction CH_2=NH, CO_2, H_2. *Phys. Chem. Chem. Phys.* **2016**, *18*, 20109–20117.

(150) Lee, H. M.; Choe, J. C. Formation of Glycine from HCN and H_2O: A Computational Mechanistic Study. *Chem. Phys. Lett.* **2017**, *675*, 6–10.

(151) Kayanuma, M.; Kidachi, K.; Shoji, M.; Komatsu, Y.; Sato, A.; Shigeta, Y. A Theoretical Study of the Formation of Glycine via Hydantoin Intermediate in Outer Space Environment. *Chem. Phys. Lett.* **2017**, *687*, 178–183.

(152) Cooper, G. W.; Cronin, J. R. Linear and Cyclic Aliphatic Carboxamides of the Murchison Meteorite: Hydrolyzable Derivatives of Amino Acids and Other Carboxylic Acids. *Geochim. Cosmochim. Acta* **1995**, *59*, 1003–1015.

(153) Shimoyama, A.; Ogasawara, R. Dipeptides and Diketopiperazines in the Yamato-791198 and Murchison Carbonaceous Chondrites. *Orig. life Evol. Biosph.* **2002**, *32*, 165–179.

(154) Vinogradoff, V.; Rimola, A.; Duvernay, F.; Danger, G.; Theulé, P.; Chiavassa, T. The Mechanism of Hexamethylenetetramine (HMT) Formation in the Solid State at Low

Temperature. *Phys. Chem. Chem. Phys.* **2012**, *14*, 12309–12320.

(155) Saladino, R.; Crestini, C.; Costanzo, G.; Negri, R.; Di Mauro, E. A Possible Prebiotic Synthesis of Purine, Adenine, Cytosine and 4 (3H)-Pyrimidinone from Formamide: Implications for the Origin of Life. *Bioorg. Med. Chem.* **2001**, *9*, 1249–1253.

(156) Saladino, R.; Ciambecchini, U.; Crestini, C.; Costanzo, G.; Negri, R.; Di Mauro, E. One-Pot TiO2-Catalyzed Synthesis of Nucleic Bases and Acylonucleosided from Formamide: Implications for the Origin of Life. *ChemBioChem* **2003**, *4*, 514–521.

(157) Saladino, R.; Crestini, C.; Costanzo, G.; Di Mauro, E. Advances in the Prebiotic Synthesis of Nucleic Acids Bases: Implications for the Origin of Life. *Curr. Org. Chem* **2004**, *8*, 1425–1443.

(158) Saladino, R.; Crestini, C.; Ciambecchini, U.; Ciciriello, F.; Costanzo, G.; Di Mauro, E. Sythesis and Degradation of Nucleobases and Nucleic Acids by Formamide in the Presence of Montmorillonites. *ChemBioChem* **2004**, *5*, 1558–1566.

(159) Saladino, R.; Crestini, C.; Neri, V.; Brucato, J. R.; Colangeli, L.; Ciciriello, F.; Di Mauro, E.; Costanzo, G. Sythesis and Degradation of Nucleobases and Nucleic Acids Components by Formamide and Cosmic Dust Analogous. *ChemBioChem* **2005**, *6*, 1368–1374.

(160) Saladino, R.; Crestini, C.; Neri, V.; Ciciriello, F.; Costanzo, G.; Di Mauro, E. Origin of Informational Polymers: The Concurrent Roles of Formamide and Phosphates. *ChemBioChem* **2006**, *7*, 1707–1714.

(161) Saladino, R.; Botta, G.; Bizzarri, B. M.; Di Mauro, E.; Garcia-Ruiz, J. M. A Global Scale Scenario for Prebiotic Chemistry: Silica-Based Self-Assembled Mineral Structures and Formamide. *Biochemistry* **2016**, *55*, 2806–2811.

(162) Rotelli, L.; Trigo-Rodríguez, J. M.; Moyano-Cambero, C. E.; Carota, E.; Botta, L.; Di Mauro, E.; Saladino, R. The Key Role of Meteorites in the Formation of Relevant Prebiotic

Molecules in a Formamide/Water Environment. *Sci. Rep.* **2016**, *6*, 38888 (7 pp).

(163) Nguyen, V. S.; Orlando, T. M.; Leszczynski, J.; Nguyen, M. T. Theoretical Study of the Decomposition of Formamide in the Presence of Water Molecules. *J. Phys. Chem. A* **2013**, *117*, 2543–2555.

(164) Wang, J.; Gu, J.; Nguyen, M. T.; Springsteen, G.; Leszczynski, J. From Formamide to Purine: A Self-Catalyzed Reaction Pathway Provides a Feasible Mechanism for the Entire Process. *J. Phys. Chem. B* **2013**, *113*, 9333–9342.

(165) Wang, J.; Gu, J.; Nguyen, M. T.; Springsteen, G.; Leszczynski, J. From Formamide to Purine: An Energetically Viable Mechanistic Reaction Pathway. *J. Phys. Chem. B* **2013**, *117*, 2314–2320.

(166) Bera, P. P.; Nuevo, M.; Milam, S. N.; Sandford, S. A.; Lee, T. J. Mechanism for the Abiotic Synthesis of Uracil via UV-Induced Oxidation of Pyrimidine in Pure H2O Ices under Astrophysical Conditions. *J. Chem. Phys.* **2010**, *133*, 104303 (7 pp).

(167) Bera, P. P.; Nuevo, M.; Materese, C. K.; Sandford, S. A.; Lee, T. J.; Bera, P. P.; Nuevo, M.; Materese, C. K.; Sandford, S. A.; Lee, T. J. Mechanisms for the Formation of Thymine under Astrophysical Conditions and Implications for the Origin of Life. *J. Chem. Phys.* **2016**, *144*, 144308 (7 pp).

(168) Bera, P. P.; Stein, T.; Head-Gordon, M.; Lee, T. J. Mechanisms of the Formation of Adenine, Guanine, and Their Analogues in UV-Irradiated Mixed NH_3:H_2O Molecular Ices Containing Purine. *Astrobiology* **2017**, *17*, 771–786.

(169) Burton, S. A.; Stern, J. C.; Elsila, J. E.; Glavin, D. P.; Dworkin, J. P. Understanding Prebiotic Chemistry through the Analysis of Extraterrestrial Amino Acids and Nucleobases in Meteorites. *Chem. Soc. Rev.* **2012**, *41*, 5459–5472.

(170) Signorile, M.; Salvini, C.; Zamirri, L.; Bonino, F.; Martra, G.; Sodupe, M.; Ugliengo, P.

Formamide Adsorption at the Amorphous Silica Surface: A Combined Experimental and Computational Approach. *Life* **2018**, *8*, 42 (13 pp).

For TOC only